



CAIF & ASI Final Report

Spacecraft Dynamics Employing a General Multi-tank and Multi-thruster Mass Depletion Formulation

Author:
Mr. Paolo PANICUCCI

Supervisor:
Dr. Hanspeter SCHAUB

Version 1.0 of
September 26, 2016

Contents

1	Introduction	4
2	Notations and reference frames	4
3	Mathematical Background	4
4	Equation of motion	5
4.1	Translational equation	5
4.2	Rotational Motion	12
4.2.1	The $[K]$ term	16
5	Fuel supply architecture and implementation	18
6	Control feedback law	19
7	Tank models	21
7.1	The constant tank's volume model	22
7.2	The constant fuel's density model	22
7.3	The emptying tank model	23
7.4	Uniform burn cylinder	26
7.5	Centrifugal burn cylinder	27
8	Thruster models	28
8.1	Impulsive model	28
8.2	Ramping model	29
9	Numerical Implementation	30
10	Results	30
10.1	Axial-symmetric rocket	30
10.1.1	Centrifugal burn	31
10.1.2	Uniform burn	31
10.2	De-tumbling maneuver	31
10.3	LEO-to-GEO maneuver	31
11	Conclusions	31

List of Figures

1	Division of the total system in spacecraft and exhausted gas. The control surface A_{exh} represents the exchanging surface between the two subsystems.	5
2	Spacecraft subsystem and main definitions.	6
3	Cases of the influence of the $[K]$ matrix on the system dynamics.	17

4	An example of the distribution system among tanks and nozzles with numerical values.	19
5	Geometrical properties of the constant density sphere.	22
6	Geometrical properties of the constant density sphere.	23
7	Geometrical properties of the emptying tank model.	24
8	Geometrical properties of the uniform burn cylinder	26
9	Geometrical properties of the centrifugal burn cylinder	27
10	Characteristics of the impulsive thruster firing from $t = 0.3$ s to $t = 0.8$ s. In the shown simulation: $I_{sp} = 400$ s and $g_0 = 9.81 \frac{m}{s^2}$.	29
11	Characteristics of the ramping thruster firing from $t = 0.3$ s to $t = 0.8$ s. In the shown simulation: $I_{sp} = 400$ s, $g_0 = 9.81 \frac{m}{s^2}$ and $\Delta t_{resp} = 50$ ms.	30

List of Tables

Acknowledgments

Abstract

Having high fidelity numerical simulations for the dynamics of a spacecraft is becoming increasingly important for space missions. Constraints are becoming more and more stringent as far as precision attitude pointing, attitude jitter, and orbital accuracy are concerned. A crucial aspect of spacecraft dynamics is the depleting mass due to thrusters. Orbital maneuvers and Dynamics and Control (ADC) nozzles firing change the current spacecraft mass properties and results in an associated reaction force and torque. To perform orbital and attitude control using thrusters, or to obtain optimal trajectories, the impact of mass variation and depletion of the spacecraft must be thoroughly understood. Earlier works make many assumptions while deriving the equations of motion, such as considering an axial symmetric body or a given tank's geometry, that could decrease the generality and applicability of the models and result in the necessity to re-derive equations of motion for specific spacecraft.

This paper develops the fully coupled translational and rotational equations of motion of a spacecraft that is ejecting mass through the use of thrusters. The derivation begins considering the entire closed system: the spacecraft and the ejected fuel. Then the exhausted fuel motion in free space is expressed using the thruster nozzle properties and the well-known thrust vector to avoid tracking the expelled fuel in the simulation. The present formulation considers a general multi-tank and multi-thruster approach to account for both the depleting fuel mass in the tanks and the one exiting the thruster nozzles. General spacecraft configurations are possible where thrusters can pull a single, multiple tanks, or the tank being drawn from can be switched via a valve.

To perform validation of the model developed and to show the impact of assumptions that are made for mass depletion in other models, numerical simulations are presented and compared to a simple parameters-update approach. Additionally, an orbital maneuver with attitude control is included and the impact on mass variation is taken into account by updating the mass flow of each ADC nozzle.

1 Introduction

2 Notations and reference frames

The following notation will be used:

- $\mathbf{r}_{C/N}$ is the vector pointing from N to C .
- ${}^{\mathcal{B}}\mathbf{r}$ is the vector \mathbf{r} expressed in the \mathcal{B} reference frame.
- $\boldsymbol{\omega}_{\mathcal{B}/\mathcal{N}}$ is the angular velocity of the \mathcal{B} reference frame about the \mathcal{N} one.
- \mathbf{r}' denotes the derivate with respect to the time in the body fixed reference frame.
- $\dot{\mathbf{r}}$ denotes the derivate with respect to the time in the \mathcal{N} reference frame.

Moreover, different reference frames will be presented to model properly the problem:

- The inertial reference frame \mathcal{N} centered in N and oriented freely in space.
- The body fixed reference frame \mathcal{B} with origin B and versors $\{\hat{\mathbf{b}}_1, \hat{\mathbf{b}}_2, \hat{\mathbf{b}}_3\}$ oriented in any direction of the space.
- \mathcal{R}
- \mathcal{M}

Finally the instantaneous satellite's center of mass will be named C , the center of mass of the spacecraft's hub will be labeled $\mathbf{r}_{Bc/B}$ and the tank's center of mass will be noted $\mathbf{r}_{Tc/B}$.

3 Mathematical Background

In this section the main tool used for the deduction of the governing equation will be presented and explained. The following theorem has always been called in the literature "Reynolds transport theorem" even if its first proof was given by Leibniz. The theorem provides a basic tool to pass from a Lagrangian formulation, based on the analysis of particles moving in space, to an Eulerian one, considering a fixed space volume where physical quantities are exchanged throughout the boundaries.

In the present document the considered Lagrangian system will be labeled *Body*, the moving volume of the Eulerian approach will be called \mathcal{V} and its surface \mathcal{A} . By using this notation, the theorem affirms [1, 2, 3, 4]:

$$\frac{d}{dt} \int_{Body} \rho \mathbf{f} dV = \frac{d}{dt} \int_{\mathcal{V}} \rho \mathbf{f} dV + \int_{\mathcal{A}} \rho \mathbf{f} (\mathbf{v}_{rel} \cdot \hat{\mathbf{n}}) dA \quad (1)$$

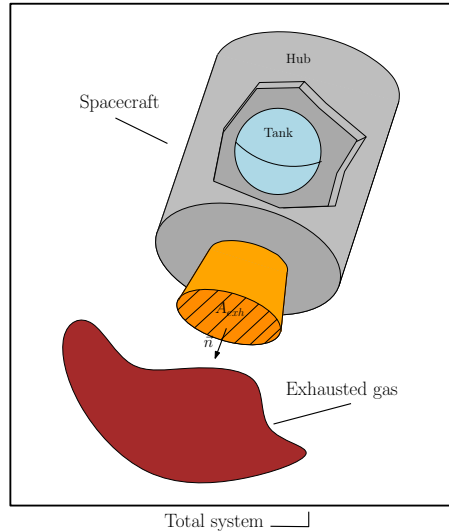


Figure 1: Division of the total system in spacecraft and exhausted gas. The control surface A_{exh} represents the exchanging surface between the two subsystems.

where \mathbf{f} is a general vectorial quantity transported out from the control volume, ρ is the density of the infinitesimal mass dm considered, $\hat{\mathbf{n}}$ the surface normal taken exiting from the control volume and \mathbf{v}_{rel} is the relative velocity of the particles exiting from the surface with respect to the control surface itself. Moreover, in the case of a non deforming control surface the following relation can be proved [2, 5] as no modification of the volume occurs:

$$\frac{d}{dt} \int_{Body} \rho \mathbf{f} dV = \int_{\mathcal{V}} \frac{d}{dt} (\rho \mathbf{f}) dV + \int_{\mathcal{A}} \rho \mathbf{f} (\mathbf{v}_{rel} \cdot \hat{\mathbf{n}}) dA \quad (2)$$

4 Equation of motion

4.1 Translational equation

The derivation of translational equation must begin considering the Newton's law for a closed system.

$$\frac{N}{dt} \int_{Body} \dot{\mathbf{r}}_{M/N} dm = \mathbf{F}_{ext} \quad (3)$$

where $\dot{\mathbf{r}}_{M/N}$ is the velocity of the particle occupying the M point expressed in the inertial reference frame and \mathbf{F}_{ext} are the external forces experienced by the point.

As the mass system is constant, the differentiation operator can be brought

inside the integration and the use the kinematics equation allows to pass from the inertial reference frame \mathcal{N} to the rotating and non-inertial \mathcal{B} :

$$\frac{\mathcal{N}d}{dt} \int_{Body} \dot{\mathbf{r}}_{M/N} dm = \int_{Body} \ddot{\mathbf{r}}_{M/N} dm \quad (4)$$

The acceleration of the origin of the \mathcal{B} frame can be expressed as:

$$\ddot{\mathbf{r}}_{M/N} = \ddot{\mathbf{r}}_{B/N} + \ddot{\mathbf{r}}_{M/B} \quad (5)$$

By using the kinematic transport theorem, the expression of $\dot{\mathbf{r}}$ can be deduced:

$$\dot{\mathbf{r}}_{M/B} = \mathbf{r}'_{M/B} + \boldsymbol{\omega}_{\mathcal{B}/\mathcal{N}} \times \mathbf{r}_{M/B} \quad (6)$$

$$\ddot{\mathbf{r}}_{M/B} = \mathbf{r}''_{M/B} + 2\boldsymbol{\omega}_{\mathcal{B}/\mathcal{N}} \times \mathbf{r}'_{M/B} + \dot{\boldsymbol{\omega}}_{\mathcal{B}/\mathcal{N}} \times \mathbf{r}_{M/B} + \boldsymbol{\omega}_{\mathcal{B}/\mathcal{N}} \times (\boldsymbol{\omega}_{\mathcal{B}/\mathcal{N}} \times \mathbf{r}_{M/B}) \quad (7)$$

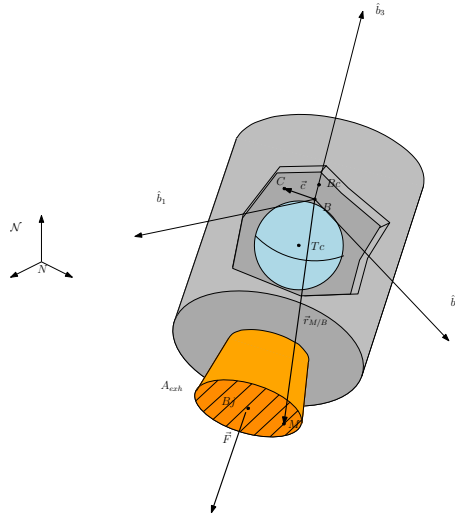


Figure 2: Spacecraft subsystem and main definitions.

A Lagrangian formulation of the linear momentum equation can be deduced by using equations 3, 4, 5 and 7:

$$\int_{Body} (\ddot{\mathbf{r}}_{B/N} + \dot{\boldsymbol{\omega}}_{\mathcal{B}/\mathcal{N}} \times \mathbf{r}_{M/B} + \boldsymbol{\omega}_{\mathcal{B}/\mathcal{N}} \times (\boldsymbol{\omega}_{\mathcal{B}/\mathcal{N}} \times \mathbf{r}_{M/B})) dm + \\ + 2\boldsymbol{\omega}_{\mathcal{B}/\mathcal{N}} \times \int_{Body} \mathbf{r}'_{M/B} dm + \int_{Body} \mathbf{r}''_{M/B} dm = \mathbf{F}_{\text{ext}} \quad (8)$$

As the system mass is constant the derivation operator can be applied before the integration. Thus:

$$\int_{Body} \mathbf{r}'_{M/B} dm = \frac{\mathcal{B}_d}{dt} \int_{Body} \mathbf{r}_{M/B} dm \quad (9)$$

$$\int_{Body} \mathbf{r}''_{M/B} dm = \frac{\mathcal{B}_d^2}{dt^2} \int_{Body} \mathbf{r}_{M/B} dm \quad (10)$$

By using the Reynolds transport theorem exposed in the previous paragraph two previous equation can be expressed in a space fixed volume shown in figure 1.

$$\frac{\mathcal{B}_d}{dt} \int_{Body} \mathbf{r}_{M/B} dm = \frac{\mathcal{B}_d}{dt} \int_{\mathcal{V}_{sc}} \rho \mathbf{r}_{M/B} d\mathcal{V} + \int_{\mathcal{A}_{sc}} \rho \mathbf{r}'_{M/B} \cdot \hat{\mathbf{n}} \mathbf{r}_{M/B} dA \quad (11)$$

$$\begin{aligned} \frac{\mathcal{B}_d^2}{dt^2} \int_{Body} \mathbf{r}_{M/B} dm &= \frac{\mathcal{B}_d^2}{dt^2} \int_{\mathcal{V}_{sc}} \rho \mathbf{r}_{M/B} d\mathcal{V} + \\ &+ \frac{\mathcal{B}_d}{dt} \int_{\mathcal{A}_{sc}} \rho \mathbf{r}'_{M/B} \cdot \hat{\mathbf{n}} \mathbf{r}_{M/B} dA + \int_{\mathcal{A}_{sc}} \rho \mathbf{r}'_{M/B} \cdot \hat{\mathbf{n}} \mathbf{r}'_{M/B} dA \end{aligned} \quad (12)$$

where $\mathbf{v}_{rel} = \mathbf{r}'_{M/B}$ because the B point is fixed with respect to the spacecraft and, clearly, the relative velocity of the particle in M is the the derivative of the position vector in the \mathcal{B} reference frame.

The equation 8 can be re-organized considering the previous relations in order to consider an Eulerian approach, i.e. based on a volume-based view.

$$\begin{aligned} &\int_{Body} (\ddot{\mathbf{r}}_{B/N} + \dot{\boldsymbol{\omega}}_{B/N} \times \mathbf{r}_{M/B} + \boldsymbol{\omega}_{B/N} \times (\boldsymbol{\omega}_{B/N} \times \mathbf{r}_{M/B})) dm + \\ &+ 2 \boldsymbol{\omega}_{B/N} \times \left(\frac{\mathcal{B}_d}{dt} \int_{\mathcal{V}_{sc}} \rho \mathbf{r}_{M/B} d\mathcal{V} + \int_{\mathcal{A}_{sc}} \rho \mathbf{r}'_{M/B} \cdot \hat{\mathbf{n}} \mathbf{r}_{M/B} dA \right) + \\ &+ \frac{\mathcal{B}_d^2}{dt^2} \int_{\mathcal{V}_{sc}} \rho \mathbf{r}_{M/B} d\mathcal{V} + \frac{\mathcal{B}_d}{dt} \int_{\mathcal{A}_{sc}} \rho \mathbf{r}'_{M/B} \cdot \hat{\mathbf{n}} \mathbf{r}_{M/B} dA + \\ &+ \int_{\mathcal{A}_{sc}} \rho \mathbf{r}'_{M/B} \cdot \hat{\mathbf{n}} \mathbf{r}'_{M/B} dA = \mathbf{F}_{ext} \end{aligned} \quad (13)$$

As explained in [1], if at the initial time all the mass is contained in the control volume the following relation stands as no mass is outside the volume of control at $t = 0$ and the quantity will be transported by the fluxes during the integration:

$$\begin{aligned} \mathbf{F}_{ext} - \int_{Body} (\ddot{\mathbf{r}}_{B/N} + \dot{\boldsymbol{\omega}}_{B/N} \times \mathbf{r}_{M/B} + \boldsymbol{\omega}_{B/N} \times (\boldsymbol{\omega}_{B/N} \times \mathbf{r}_{M/B})) dm = \\ = \int_{\mathcal{V}_{sc}} d\mathbf{F}_{vol} + \int_{\mathcal{A}_{sc}} d\mathbf{F}_{surf} - \int_{\mathcal{V}_{sc}} \rho (\ddot{\mathbf{r}}_{B/N} + \dot{\boldsymbol{\omega}}_{B/N} \times \mathbf{r}_{M/B} + \\ + \boldsymbol{\omega}_{B/N} \times (\boldsymbol{\omega}_{B/N} \times \mathbf{r}_{M/B})) d\mathcal{V} \end{aligned} \quad (14)$$

where the forces has been divided on the volumetric ones and the ones applied on the spacecraft surface.

Thus:

$$\begin{aligned}
& \int_{\mathcal{V}_{sc}} \rho \left(\ddot{\mathbf{r}}_{B/N} + \dot{\boldsymbol{\omega}}_{B/N} \times \mathbf{r}_{M/B} + \boldsymbol{\omega}_{B/N} \times (\boldsymbol{\omega}_{B/N} \times \mathbf{r}_{M/B}) \right) d\mathcal{V} + \\
& + 2 \boldsymbol{\omega}_{B/N} \times \left(\frac{\mathcal{B}_d}{dt} \int_{\mathcal{V}_{sc}} \rho \mathbf{r}_{M/B} d\mathcal{V} + \int_{\mathcal{A}_{sc}} \rho \mathbf{r}'_{M/B} \cdot \hat{\mathbf{n}} \mathbf{r}_{M/B} dA \right) + \\
& + \frac{\mathcal{B}_d^2}{dt^2} \int_{\mathcal{V}_{sc}} \rho \mathbf{r}_{M/B} d\mathcal{V} + \frac{\mathcal{B}_d}{dt} \int_{\mathcal{A}_{sc}} \rho \mathbf{r}'_{M/B} \cdot \hat{\mathbf{n}} \mathbf{r}_{M/B} dA + \\
& + \int_{\mathcal{A}_{sc}} \rho \mathbf{r}'_{M/B} \cdot \hat{\mathbf{n}} \mathbf{r}'_{M/B} dA = \int_{\mathcal{V}_{sc}} d\mathbf{F}_{vol} + \int_{\mathcal{A}_{sc}} d\mathbf{F}_{surf} \quad (15)
\end{aligned}$$

As the present paper aims to introduce the dynamic's equations in case of varying mass inside the spacecraft, two point must be developed: on one hand both the translational equation and the rotational one will be expressed with the vector $\mathbf{r}_{B/N}$ as free variable and, on the other, a complete and comprehensive model of the $\mathbf{c} = \mathbf{r}_{C/B}$ vector must be performed in order to follow the instantaneous displacement of the center of mass all along the trajectory of the satellite.

Calculating the satellite's center of mass in the \mathcal{B} reference frame, the \mathbf{c} vector can be expressed with respect to the masses of each component of the satellite.

$$\mathbf{c} = \frac{m_{hub} \mathbf{r}_{Bc/B} + \sum_{i=1}^M m_{fuel_i} \mathbf{r}_{Fc_i/B}}{m_{hub} + \sum_{i=1}^M m_{fuel_i}} \quad (16)$$

where m_{hub} is the hub mass, m_{fuel_i} the i -th fuel mass and $\mathbf{r}_{Fc_i/B}$ the position of the i -th fuel's center of mass.

In order to infer the influence of the mass variation in the equation of motion the relation 16 must be derived. Thus, in the \mathcal{B} frame:

$$\begin{aligned}
\mathbf{c}' = & \frac{\sum_{i=1}^M \left(\dot{m}_{fuel_i} \mathbf{r}_{Fc_i/B} + m_{fuel_i} \mathbf{r}'_{Fc_i/B} \right)}{m_{hub} + \sum_{i=1}^M m_{fuel_i}} + \\
& - \frac{\left(\sum_{i=1}^M \dot{m}_{fuel_i} \right) \left(m_{hub} \mathbf{r}_{Bc/B} + \sum_{i=1}^M m_{fuel_i} \mathbf{r}_{Fc_i/B} \right)}{\left(m_{hub} + \sum_{i=1}^M m_{fuel_i} \right)^2} \quad (17)
\end{aligned}$$

$$\begin{aligned}
\mathbf{c}'' = & \frac{\sum_{i=1}^M \left(\ddot{m}_{\text{fuel}_i} \mathbf{r}_{F_{c_i}/B} + 2 \dot{m}_{\text{fuel}_i} \mathbf{r}'_{F_{c_i}/B} + m_{\text{fuel}_i} \mathbf{r}''_{F_{c_i}/B} \right)}{m_{\text{hub}} + \sum_{i=1}^M m_{\text{fuel}_i}} + \\
& - \frac{\left(\sum_{i=1}^M \ddot{m}_{\text{fuel}_i} \right) \left(m_{\text{hub}} \mathbf{r}_{Bc/B} + \sum_{i=1}^M m_{\text{fuel}_i} \mathbf{r}_{F_{c_i}/B} \right)}{\left(m_{\text{hub}} + \sum_{i=1}^M m_{\text{fuel}_i} \right)^2} + \\
& - \frac{2 \left(\sum_{i=1}^M \dot{m}_{\text{fuel}_i} \right) \sum_{i=1}^M \left(\dot{m}_{\text{fuel}_i} \mathbf{r}_{F_{c_i}/B} + m_{\text{fuel}_i} \mathbf{r}'_{F_{c_i}/B} \right)}{\left(m_{\text{hub}} + \sum_{i=1}^M m_{\text{fuel}_i} \right)^2} + \\
& + \frac{2 \left(\sum_{i=1}^M \dot{m}_{\text{fuel}_i} \right)^2 \left(m_{\text{hub}} \mathbf{r}_{Bc/B} + \sum_{i=1}^M m_{\text{fuel}_i} \mathbf{r}_{F_{c_i}/B} \right)}{\left(m_{\text{hub}} + \sum_{i=1}^M m_{\text{fuel}_i} \right)^3} \quad (18)
\end{aligned}$$

Once the vector \mathbf{c} has been evaluated, the completed translational equation of motion can be simplified both assuming no relative internal mass flow inside the reference volume and expressing each term with respect to nozzle's position and geometric feature of each thruster.

In the following pages the terms of equation 15 will be analyzed in order to have a simpler relation adapted to the case under study. The main hypothesis that will be taken into account are:

- The body is rigid and deformation are not considered.
- The mass flow inside among the tanks and the thrusters is considered to be a second order effect and, thus, neglected.
- The particles are accelerated instantaneously from the spacecraft velocity to the exhausted velocity at the nozzle surface.
- The particle exhausted velocity \mathbf{v}_{exh} is considered constant and parallel to the nozzle's normal $\hat{\mathbf{n}}$

The first integral in equation 15 is the easiest to compute tanking into account that $\mathbf{r}_{M/B} = \mathbf{c} + \mathbf{r}_{M/C}$ and the definition of barycenter:

$$\begin{aligned}
\int_{\mathcal{V}_{\text{sc}}} \rho \left(\ddot{\mathbf{r}}_{B/N} + \dot{\boldsymbol{\omega}}_{B/N} \times \mathbf{r}_{M/B} + \boldsymbol{\omega}_{B/N} \times (\boldsymbol{\omega}_{B/N} \times \mathbf{r}_{M/B}) \right) d\mathcal{V} = \\
= m_{\text{sc}} \ddot{\mathbf{r}}_{B/N} + m_{\text{sc}} \dot{\boldsymbol{\omega}}_{B/N} \times \mathbf{c} + m_{\text{sc}} \boldsymbol{\omega}_{B/N} \times (\boldsymbol{\omega}_{B/N} \times \mathbf{c}) \quad (19)
\end{aligned}$$

where $m_{\text{sc}} = m_{\text{hub}} + \sum_{i=1}^M m_{\text{fuel}_i}$ is the instantaneous mass of the spacecraft. AS far as the second and the fourth integral concern, their expression using the considered variable can be performed throughout the definition of barycenter and decomposing the vector $\mathbf{r}_{M/B}$. Thus:

$$\frac{\mathcal{B}_d}{dt} \int_{\mathcal{V}_{sc}} \rho \mathbf{r}_{M/B} d\mathcal{V} = \frac{\mathcal{B}_d}{dt} (m_{sc} \mathbf{c}) = m_{sc} \mathbf{c}' + \dot{m}_{fuel} \mathbf{c} \quad (20)$$

where $\dot{m}_{fuel} = \sum_{i=1}^M \dot{m}_{fuel_i}$.

$$\frac{\mathcal{B}_d^2}{dt^2} \int_{\mathcal{V}_{sc}} \rho \mathbf{r}_{M/B} d\mathcal{V} = \frac{\mathcal{B}_d^2}{dt^2} (m_{sc} \mathbf{c}) = m_{sc} \mathbf{c}'' + 2 \dot{m}_{fuel} \mathbf{c}' + \ddot{m}_{fuel} \mathbf{c} \quad (21)$$

where $\ddot{m}_{fuel} = \sum_{i=1}^M \ddot{m}_{fuel_i}$.

In order to infer the term calculated on the reference surface, i.e. the third, the fifth and the sixth integrals, it could be convenient to separate the integral on the surface of each nozzle and then sum them up. Moreover, as the fuel's properties are flowing out from a spherical surface, it is convenient to express the vector $\mathbf{r}_{M/B}$ as follows $\mathbf{r}_{M/B} = \mathbf{r}_{M/Fc_j} + \mathbf{r}_{Fc_j/B}$ where Fc_i is the area barycenter. Finally, a convenient variable transformation can be performed to compute the properties exchanged while the mass disk is passing through the reference surface $d\dot{m} = -\rho \mathbf{r}'_{M/B} \cdot \hat{\mathbf{n}} dA$.

$$\begin{aligned} \int_{\mathcal{A}_{sc}} \rho \mathbf{r}'_{M/B} \cdot \hat{\mathbf{n}} \mathbf{r}_{M/B} dA &= \sum_{j=1}^N \int_{\mathcal{A}_{noz_j}} \rho \mathbf{r}'_{M/B} \cdot \mathbf{n} \mathbf{r}_{M/B} dA = \\ &= - \sum_{j=1}^N \int_{\dot{m}_{noz_j}} (\mathbf{r}_{M/N_j} + \mathbf{r}_{N_j/B}) d\dot{m} = - \sum_{j=1}^N \dot{m}_{noz_j} \mathbf{r}_{N_j/B} \end{aligned} \quad (22)$$

where the first part of the integral is null because of barycenter definition and \dot{m}_{noz_j} is the mass flow of the j -th nozzle.

$$\begin{aligned} \frac{\mathcal{B}_d}{dt} \int_{\mathcal{A}_{sc}} \rho \mathbf{r}'_{M/B} \cdot \hat{\mathbf{n}} \mathbf{r}_{M/B} dA &= \frac{\mathcal{B}_d}{dt} \left(- \sum_{j=1}^N \dot{m}_{noz_j} \mathbf{r}_{N_j/B} \right) = \\ &= - \sum_{j=1}^N \left(\ddot{m}_{noz_j} \mathbf{r}_{N_j/B} + \dot{m}_{noz_j} \mathbf{r}'_{N_j/B} \right) = - \sum_{j=1}^N \ddot{m}_{noz_j} \mathbf{r}_{N_j/B} \end{aligned} \quad (23)$$

where the last equivalence stands as the nozzle barycenter is motionless with respect to the body-fixed point B and \ddot{m}_{noz_j} is the mass flow derivative of the j -th nozzle.

The sixth integral can be easily solved if the exhausted velocity $\mathbf{r}'_{M/B} = \mathbf{v}_{exh}$ is considered constant at the nozzle's exit, as previously hypothesized.

$$\begin{aligned} \int_{\mathcal{A}_{sc}} \rho \mathbf{r}'_{M/B} \cdot \hat{\mathbf{n}} \mathbf{r}'_{M/B} dA &= \sum_{j=1}^N \int_{\mathcal{A}_{noz_j}} \rho \mathbf{r}'_{M/B} \cdot \mathbf{n} \mathbf{r}'_{M/B} dA = \\ &= - \sum_{j=1}^N \int_{\dot{m}_{noz_j}} \mathbf{v}_{exh} d\dot{m} = - \sum_{j=1}^N \dot{m}_{noz_j} \mathbf{v}_{exh_j} \end{aligned} \quad (24)$$

where $\mathbf{v}_{\text{exh}_j}$ is the exhausted velocity of a particle exiting from the j -th nozzle. Finally the two integrals of the right member of equation 15 can easily be computed once a force model is chosen. This step depends directly from the problem under study. As the present work aims to provide general spacecraft rotational and translational equations, the only term that can be developed analytically is the surfacing integral in order to take into account the effect of the pressure jump between the nozzle and the environment. Thus:

$$\int_{\mathcal{V}_{\text{sc}}} d\mathbf{F}_{\text{vol}} + \int_{\mathcal{A}_{\text{sc}}} d\mathbf{F}_{\text{surf}} = \mathbf{F}_{\text{ext, vol}} + \mathbf{F}_{\text{ext, surf}} + \sum_{j=1}^N \frac{\mathbf{v}_{\text{exh}_j}}{v_{\text{exh}_j}} A_{\text{noz}_j} (p_{\text{exh}_j} - p_{\text{atm}}) \quad (25)$$

where $\mathbf{F}_{\text{ext, vol}}$ are the external forces acting on the control volume, $\mathbf{F}_{\text{ext, surf}}$ are the external forces accelerating the control surface, p_{exh_j} is the particles' exhausted pressure at the j -th nozzle and p_{atm} is the atmospheric pressure at the flying altitude.

Finally, the equation 15 can be rewritten considering nozzles' geometry and fluid properties by using equations 20, 21, 22, 23, 24, 25.

$$\begin{aligned} & m_{\text{sc}} \ddot{\mathbf{r}}_{B/N} + m_{\text{sc}} \dot{\boldsymbol{\omega}}_{B/N} \times \mathbf{c} + m_{\text{sc}} \boldsymbol{\omega}_{B/N} \times (\boldsymbol{\omega}_{B/N} \times \mathbf{c}) + m_{\text{sc}} \mathbf{c}'' + 2 \dot{m}_{\text{fuel}} \mathbf{c}' + \\ & + \ddot{m}_{\text{fuel}} \mathbf{c} + 2 \boldsymbol{\omega}_{B/N} \times \left(m_{\text{sc}} \mathbf{c}' + \dot{m}_{\text{fuel}} \mathbf{c} - \sum_{j=1}^N \dot{m}_{\text{noz}_j} \mathbf{r}_{N_j/B} \right) - \sum_{j=1}^N \ddot{m}_{\text{noz}_j} \mathbf{r}_{N_j/B} + \\ & - \sum_{j=1}^N \dot{m}_{\text{noz}_j} \mathbf{v}_{\text{exh}_j} = \mathbf{F}_{\text{ext, vol}} + \mathbf{F}_{\text{ext, surf}} + \sum_{j=1}^N \frac{\mathbf{v}_{\text{exh}_j}}{v_{\text{exh}_j}} A_{\text{noz}_j} (p_{\text{exh}_j} - p_{\text{atm}}) \quad (26) \end{aligned}$$

where \mathbf{c} , \mathbf{c}' , \mathbf{c}'' have been specified in equations 16, 18, 19.

The previous equation can be righted by defining the following quantity:

$$\mathbf{F}_{\text{thr}_j} = \mathbf{v}_{\text{exh}_j} \left(\frac{A_{\text{noz}_j}}{v_{\text{exh}_j}} (p_{\text{exh}_j} - p_{\text{atm}}) + \dot{m}_{\text{noz}_j} \right) = I_{\text{sp}_j} g_0 \dot{m}_{\text{noz}_j} \frac{\mathbf{v}_{\text{exh}_j}}{v_{\text{exh}_j}} \quad (27)$$

Thus:

$$\begin{aligned} \ddot{\mathbf{r}}_{B/N} - \mathbf{c} \times \dot{\boldsymbol{\omega}}_{B/N} &= + \frac{1}{m_{\text{sc}}} \sum_{j=1}^N \mathbf{F}_{\text{thr}_j} - 2 \frac{\dot{m}_{\text{fuel}}}{m_{\text{sc}}} (\mathbf{c}' + \boldsymbol{\omega}_{B/N} \times \mathbf{c}) - \mathbf{c}'' + \\ & - 2 \boldsymbol{\omega}_{B/N} \times \mathbf{c}' - \boldsymbol{\omega}_{B/N} \times (\boldsymbol{\omega}_{B/N} \times \mathbf{c}) + \frac{2}{m_{\text{sc}}} \sum_{j=1}^N \dot{m}_{\text{noz}_j} \boldsymbol{\omega}_{B/N} \times \mathbf{r}_{N_j/B} + \\ & + \frac{1}{m_{\text{sc}}} \sum_{j=1}^N \ddot{m}_{\text{noz}_j} \mathbf{r}_{N_j/B} - \ddot{m}_{\text{fuel}} \mathbf{c} + \frac{1}{m_{\text{sc}}} \mathbf{F}_{\text{ext, vol}} + \frac{1}{m_{\text{sc}}} \mathbf{F}_{\text{ext, surf}} \quad (28) \end{aligned}$$

Moreover, if the cross product is substituted with the skew matrix associated, the translational equation 28 can be written in a more compact form:

$$\begin{aligned}
\ddot{\mathbf{r}}_{B/N} + [\tilde{\mathbf{c}}]^T \dot{\boldsymbol{\omega}}_{B/N} = & + \frac{1}{m_{sc}} \sum_{j=1}^N \mathbf{F}_{thr_j} - 2 \frac{\dot{m}_{fuel}}{m_{sc}} (\mathbf{c}' + [\tilde{\boldsymbol{\omega}}_{B/N}] \times \mathbf{c}) - \mathbf{c}'' + \\
& + 2 [\tilde{\boldsymbol{\omega}}_{B/N}]^T \mathbf{c}' + [\tilde{\boldsymbol{\omega}}_{B/N}]^T [\tilde{\boldsymbol{\omega}}_{B/N}] \mathbf{c} + \frac{2}{m_{sc}} \sum_{j=1}^N \dot{m}_{noz_j} [\tilde{\boldsymbol{\omega}}_{B/N}] \mathbf{r}_{N_j/B} + \\
& + \frac{1}{m_{sc}} \sum_{j=1}^N \ddot{m}_{noz_j} \mathbf{r}_{F_{c_j/B}} - \ddot{m}_{fuel} \mathbf{c} + \frac{1}{m_{sc}} \mathbf{F}_{ext, vol} + \frac{1}{m_{sc}} \mathbf{F}_{ext, surf} \quad (29)
\end{aligned}$$

This equation of motion is the Newton's law for an open system subjected to external forces $\mathbf{F}_{ext, vol} + \mathbf{F}_{ext, surf}$ and thrust $\mathbf{F}_{thr} = \sum_{j=1}^N \mathbf{F}_{thr_j}$ due to mass depletion of the spacecraft, represented in figure 2. From this equation can be deduced that the variation of the mass inside the spacecraft affect directly the position of the satellite itself with respect to the origin as the body fixed point B changes its state of motion according to the variation of the tanks' linear inertia.

4.2 Rotational Motion

In this section the rotational equation of motion will be developed taking into account the variation of fuel in the reservoirs. Beginning from the Newton's equation and calling M the point where the infinitesimal mass dm is:

$$\ddot{\mathbf{r}}_{M/N} dm = d\mathbf{F} \quad \Rightarrow \quad \mathbf{r}_{M/N} \times \ddot{\mathbf{r}}_{M/N} dm = \mathbf{r}_{M/N} \times d\mathbf{F} \quad (30)$$

By performing an integration all over the system:

$$\int_{Body} \mathbf{r}_{M/N} \times \ddot{\mathbf{r}}_{M/N} dm = \int_{Body} \mathbf{r}_{M/N} \times d\mathbf{F} \quad (31)$$

The left term of the equation can be manipulated in order to consider a different reference of the origin of the momentum equation thanks to kinematics identities:

$$\begin{aligned}
\int_{Body} \rho \mathbf{r}_{M/N} \times \ddot{\mathbf{r}}_{M/N} d\mathcal{V} = & \int_{Body} \rho \mathbf{r}_{M/B} \times \ddot{\mathbf{r}}_{M/B} d\mathcal{V} + \\
+ \int_{Body} \rho \mathbf{r}_{B/N} \times \ddot{\mathbf{r}}_{M/N} d\mathcal{V} + & \int_{Body} \rho \mathbf{r}_{M/B} \times \ddot{\mathbf{r}}_{B/N} d\mathcal{V} = \int_{Body} \mathbf{r}_{M/N} \times d\mathbf{F} \quad (32)
\end{aligned}$$

Considering that $\ddot{\mathbf{r}}_{M/N} dm = d\mathbf{F}$, the torque caused by the forces acting on the body can be easily defined:

$$\begin{aligned}
& \int_{Body} \mathbf{r}_{M/N} \times d\mathbf{F} - \int_{Body} \rho \mathbf{r}_{B/N} \times \ddot{\mathbf{r}}_{M/N} d\mathcal{V} = \\
& = \int_{Body} (\mathbf{r}_{M/N} - \mathbf{r}_{B/N}) \times \ddot{\mathbf{r}}_{M/N} d\mathbf{F} = \int_{Body} \mathbf{r}_{M/B} \times \ddot{\mathbf{r}}_{M/N} d\mathbf{F} = \mathbf{L}_B \quad (33)
\end{aligned}$$

where \mathbf{L}_B is the torque with respect to the body-fixed point B .

As the mass of the system is constant, the derivative of the angular momentum about point B can be inferred easily from equation 32 thanks to the property of the cross product and the previously exposed Reynold transport theorem:

$$\begin{aligned}
\int_{Body} \rho \mathbf{r}_{M/B} \times \ddot{\mathbf{r}}_{M/B} d\mathcal{V} &= \frac{\mathcal{N}d}{dt} \int_{\mathcal{V}_{sc}} \rho \mathbf{r}_{M/B} \times \dot{\mathbf{r}}_{M/B} d\mathcal{V} + \\
&+ \int_{\mathcal{A}_{sc}} \rho \mathbf{r}'_{M/B} \cdot \hat{\mathbf{n}} (\mathbf{r}_{M/B} \times \dot{\mathbf{r}}_{M/B}) dA \quad (34)
\end{aligned}$$

Moreover, as in the translational equation, if all the mass of the system is contained at the initial time inside the control volume, the following relation stands:

$$\begin{aligned}
\int_{Body} \rho \mathbf{r}_{M/B} \times \ddot{\mathbf{r}}_{B/N} d\mathcal{V} - \mathbf{L}_B &= \int_{\mathcal{V}_{sc}} \rho \mathbf{r}_{M/B} \times \ddot{\mathbf{r}}_{B/N} d\mathcal{V} - \int_{\mathcal{V}_{sc}} \mathbf{r}_{M/B} \times d\mathbf{F}_{vol} + \\
&- \int_{\mathcal{A}_{sc}} \mathbf{r}_{M/B} \times d\mathbf{F}_{surf} = m_{sc} \mathbf{c} \times \ddot{\mathbf{r}}_{B/N} - \mathbf{L}_{B, vol} - \mathbf{L}_{B, surf} \quad (35)
\end{aligned}$$

where $\mathbf{L}_{B, vol}$ and $\mathbf{L}_{B, surf}$ are the torque caused by the volume forces and surface one respectively.

Finally, the general rotational equation for a control volume in a rotating reference frame can be reorganized:

$$\begin{aligned}
\dot{\mathbf{H}}_{sc, B} + \int_{\mathcal{A}_{sc}} \rho \mathbf{r}'_{M/B} \cdot \hat{\mathbf{n}} (\mathbf{r}_{M/B} \times \dot{\mathbf{r}}_{M/B}) dA + m_{sc} \mathbf{c} \times \ddot{\mathbf{r}}_{B/N} &= \\
&= \mathbf{L}_{B, vol} + \mathbf{L}_{B, surf} \quad (36)
\end{aligned}$$

By definition of angular momentum vector about point B :

$$\begin{aligned}
\mathbf{H}_{sc, B} &= [I_{hub, Bc}] \boldsymbol{\omega}_{B/N} + \mathbf{r}_{Bc/B} \times m_{hub} \dot{\mathbf{r}}_{Bc/B} + \\
&+ \sum_{i=1}^M ([I_{fuel_i, Fc_i}] \boldsymbol{\omega}_{B/N} + \mathbf{r}_{Fc_i/B} \times m_{fuel_i} \dot{\mathbf{r}}_{Fc_i/B}) \quad (37)
\end{aligned}$$

where $[I_{hub, Bc}]$ is the hub's inertia about its center of mass Bc .

Furthermore, an analytical expression of the mass variation influence on the rotational motion can be deduced:

$$\begin{aligned}
\dot{\mathbf{H}}_{\text{sc}, B} = & [I_{\text{hub}, Bc}] \dot{\boldsymbol{\omega}}_{\mathcal{B}/\mathcal{N}} + \boldsymbol{\omega}_{\mathcal{B}/\mathcal{N}} \times ([I_{\text{hub}, Bc}] \boldsymbol{\omega}_{\mathcal{B}/\mathcal{N}}) + \mathbf{r}_{Bc/B} \times m_{\text{hub}} \ddot{\mathbf{r}}_{Bc/B} + \\
& + \sum_{i=1}^M ([I_{\text{fuel}_i, Fc_i}] \dot{\boldsymbol{\omega}}_{\mathcal{B}/\mathcal{N}} + \boldsymbol{\omega}_{\mathcal{B}/\mathcal{N}} \times ([I_{\text{fuel}_i, Fc_i}] \boldsymbol{\omega}_{\mathcal{B}/\mathcal{N}}) + \mathbf{r}_{Fc_i/B} \times m_{\text{fuel}_i} \ddot{\mathbf{r}}_{Fc_i/B} + \\
& + \mathbf{r}_{Fc_i/B} \times \dot{m}_{\text{fuel}_i} \dot{\mathbf{r}}_{Fc_i/B} + [I_{\text{fuel}_i, Fc_i}]' \boldsymbol{\omega}_{\mathcal{B}/\mathcal{N}}) \quad (38)
\end{aligned}$$

It must be noticed that no relative motion of the particle inside the spacecraft has been considered and, as a consequence, there is no effect both of the Coriolis' acceleration and of the whirling motion on the spacecraft dynamics. An more detailed dissertation of the impact of these effect on the spacecraft can be found in [6].

Additionally, the derivate of the vectors $\mathbf{r}_{Bc/B}$ and $\mathbf{r}_{Fc_i/B}$ can be computed using the transport theorem between the two reference frames:

$$\dot{\mathbf{r}}_{Bc/B} = \mathbf{r}'_{Bc/B} + \boldsymbol{\omega}_{\mathcal{B}/\mathcal{N}} \times \mathbf{r}_{Bc/B} = \boldsymbol{\omega}_{\mathcal{B}/\mathcal{N}} \times \mathbf{r}_{Bc/B} \quad (39)$$

$$\ddot{\mathbf{r}}_{Bc/B} = \dot{\boldsymbol{\omega}}_{\mathcal{B}/\mathcal{N}} \times \mathbf{r}_{Bc/B} + \boldsymbol{\omega}_{\mathcal{B}/\mathcal{N}} \times (\boldsymbol{\omega}_{\mathcal{B}/\mathcal{N}} \times \mathbf{r}_{Bc/B}) \quad (40)$$

$$\dot{\mathbf{r}}_{Fc_i/B} = \mathbf{r}'_{Fc_i/B} + \boldsymbol{\omega}_{\mathcal{B}/\mathcal{N}} \times \mathbf{r}_{Fc_i/B} \quad (41)$$

$$\begin{aligned}
\ddot{\mathbf{r}}_{Fc_i/B} = & \mathbf{r}''_{Fc_i/B} + 2 \boldsymbol{\omega}_{\mathcal{B}/\mathcal{N}} \times \mathbf{r}'_{Fc_i/B} + \dot{\boldsymbol{\omega}}_{\mathcal{B}/\mathcal{N}} \times \mathbf{r}_{Fc_i/B} + \\
& + \boldsymbol{\omega}_{\mathcal{B}/\mathcal{N}} \times (\boldsymbol{\omega}_{\mathcal{B}/\mathcal{N}} \times \mathbf{r}_{Fc_i/B}) \quad (42)
\end{aligned}$$

By substituting equations 40, 41 and 42 in equation 38 can be rewritten:

$$\begin{aligned}
\dot{\mathbf{H}}_{\text{sc}, B} = & [I_{\text{hub}, Bc}] \dot{\boldsymbol{\omega}}_{\mathcal{B}/\mathcal{N}} + \boldsymbol{\omega}_{\mathcal{B}/\mathcal{N}} \times ([I_{\text{hub}, Bc}] \boldsymbol{\omega}_{\mathcal{B}/\mathcal{N}}) + \\
& + \mathbf{r}_{Bc/B} \times m_{\text{hub}} (\dot{\boldsymbol{\omega}}_{\mathcal{B}/\mathcal{N}} \times \mathbf{r}_{Bc/B} + \boldsymbol{\omega}_{\mathcal{B}/\mathcal{N}} \times (\boldsymbol{\omega}_{\mathcal{B}/\mathcal{N}} \times \mathbf{r}_{Bc/B})) + \\
& + \sum_{i=1}^M ([I_{\text{fuel}_i, Fc_i}] \dot{\boldsymbol{\omega}}_{\mathcal{B}/\mathcal{N}} + \boldsymbol{\omega}_{\mathcal{B}/\mathcal{N}} \times ([I_{\text{fuel}_i, Fc_i}] \boldsymbol{\omega}_{\mathcal{B}/\mathcal{N}}) + \\
& + \mathbf{r}_{Fc_i/B} \times m_{\text{fuel}_i} (\mathbf{r}''_{Fc_i/B} + 2 \boldsymbol{\omega}_{\mathcal{B}/\mathcal{N}} \times \mathbf{r}'_{Fc_i/B} + \\
& + \dot{\boldsymbol{\omega}}_{\mathcal{B}/\mathcal{N}} \times \mathbf{r}_{Fc_i/B} + \boldsymbol{\omega}_{\mathcal{B}/\mathcal{N}} \times (\boldsymbol{\omega}_{\mathcal{B}/\mathcal{N}} \times \mathbf{r}_{Fc_i/B})) + \\
& + \mathbf{r}_{Fc_i/B} \times \dot{m}_{\text{fuel}_i} (\mathbf{r}'_{Fc_i/B} + \boldsymbol{\omega}_{\mathcal{B}/\mathcal{N}} \times \mathbf{r}_{Fc_i/B}) + [I_{\text{fuel}_i, Fc_i}]' \boldsymbol{\omega}_{\mathcal{B}/\mathcal{N}}) \quad (43)
\end{aligned}$$

In order to compact the equation 43 the following inertia matrices must be defined using the tilde operator to replace the cross product:

$$[I_{\text{hub}, B}] = [I_{\text{hub}, Bc}] + m_{\text{hub}} [\tilde{\mathbf{r}}_{Bc/B}] [\tilde{\mathbf{r}}_{Bc/B}]^T \quad (44)$$

$$[I_{\text{fuel}_i, B}] = [I_{\text{fuel}_i, Fc_i}] + m_{\text{fuel}_i} [\tilde{\mathbf{r}}_{Fc_i/B}] [\tilde{\mathbf{r}}_{Fc_i/B}]^T \quad (45)$$

$$[I_{\text{sc}, B}] = [I_{\text{hub}, B}] + \sum_{i=1}^M [I_{\text{fuel}_i, B}] \quad (46)$$

Moreover, using the Jacobi identity for the cross product $\mathbf{a} \times (\mathbf{b} \times \mathbf{c}) + \mathbf{b} \times (\mathbf{c} \times \mathbf{a}) + \mathbf{c} \times (\mathbf{a} \times \mathbf{b}) = \mathbf{0}$ the derivative of the fuel inertia in the \mathcal{B} reference frame can be introduced:

$$\begin{aligned} \mathbf{r}_{F_{c_i}/B} \times \left(2\boldsymbol{\omega}_{\mathcal{B}/\mathcal{N}} \times \mathbf{r}'_{F_{c_i}/B} \right) &= -\mathbf{r}_{F_{c_i}/B} \times \left(\mathbf{r}'_{F_{c_i}/B} \times \boldsymbol{\omega}_{\mathcal{B}/\mathcal{N}} \right) + \\ &+ \mathbf{r}_{F_{c_i}/B} \times \left(\boldsymbol{\omega}_{\mathcal{B}/\mathcal{N}} \times \mathbf{r}'_{F_{c_i}/B} \right) = -\mathbf{r}_{F_{c_i}/B} \times \left(\mathbf{r}'_{F_{c_i}/B} \times \boldsymbol{\omega}_{\mathcal{B}/\mathcal{N}} \right) + \\ &- \mathbf{r}'_{F_{c_i}/B} \times \left(\mathbf{r}_{F_{c_i}/B} \times \boldsymbol{\omega}_{\mathcal{B}/\mathcal{N}} \right) + \boldsymbol{\omega}_{\mathcal{B}/\mathcal{N}} \times \left(\mathbf{r}_{F_{c_i}/B} \times \mathbf{r}'_{F_{c_i}/B} \right) \end{aligned} \quad (47)$$

$$\begin{aligned} [I_{\text{fuel}_i, B}]' &= [I_{\text{fuel}_i, F_{c_i}}] + \dot{m}_{\text{fuel}_i} [\tilde{\mathbf{r}}_{F_{c_i}/B}] [\tilde{\mathbf{r}}_{F_{c_i}/B}]^T + \\ &+ m_{\text{fuel}_i} \left([\tilde{\mathbf{r}}_{F_{c_i}/B}] [\tilde{\mathbf{r}}'_{F_{c_i}/B}]^T + [\tilde{\mathbf{r}}'_{F_{c_i}/B}] [\tilde{\mathbf{r}}_{F_{c_i}/B}]^T \right) \end{aligned} \quad (48)$$

Thus, by substituting equations 44, 45, 46, 47 and 48 and developing the expressions:

$$\begin{aligned} \dot{\mathbf{H}}_{\text{sc}, B} &= [I_{\text{sc}, B}] \dot{\boldsymbol{\omega}}_{\mathcal{B}/\mathcal{N}} + [\tilde{\boldsymbol{\omega}}_{\mathcal{B}/\mathcal{N}}] [I_{\text{sc}, B}] \boldsymbol{\omega}_{\mathcal{B}/\mathcal{N}} + \sum_{i=1}^M \left(m_{\text{fuel}_i} [\tilde{\mathbf{r}}_{F_{c_i}/B}] \mathbf{r}''_{F_{c_i}/B} + \right. \\ &\left. + \dot{m}_{\text{fuel}_i} [\tilde{\mathbf{r}}_{F_{c_i}/B}] \mathbf{r}'_{F_{c_i}/B} + [I_{\text{fuel}_i, B}]' \boldsymbol{\omega}_{\mathcal{B}/\mathcal{N}} + [\tilde{\boldsymbol{\omega}}_{\mathcal{B}/\mathcal{N}}] [\tilde{\mathbf{r}}_{F_{c_i}/B}] \mathbf{r}'_{F_{c_i}/B} \right) \end{aligned} \quad (49)$$

Considering that, at the nozzles's exit, $\dot{\mathbf{r}}_{M/B} = \mathbf{v}_{\text{exh}_j} + \boldsymbol{\omega}_{\mathcal{B}/\mathcal{N}} \times \mathbf{r}_{M/B}$ and $d\dot{m} = -\rho \mathbf{r}'_{M/B} \cdot \hat{\mathbf{n}} dA$, the surface integral can be expressed in term of the nozzles' surface:

$$\begin{aligned} \int_{A_{\text{exh}}} \rho \mathbf{r}'_{M/B} \cdot \mathbf{n} (\mathbf{r}_{M/B} \times \dot{\mathbf{r}}_{M/B}) dA &= - \sum_{j=1}^N \int_{\dot{m}_{\text{noz}_j}} \mathbf{r}_{M/B} \times \mathbf{v}_{\text{exh}_j} d\dot{m} + \\ &+ \sum_{j=1}^N \int_{\dot{m}_{\text{noz}_j}} \mathbf{r}_{M/B} \times (\mathbf{r}_{M/B} \times \boldsymbol{\omega}_{\mathcal{B}/\mathcal{N}}) d\dot{m} \end{aligned} \quad (50)$$

Finally the equation of motion 36 can be updated using equations 49 and 50:

$$\begin{aligned} \dot{\mathbf{H}}_{\text{sc}, B} &= [I_{\text{sc}, B}] \dot{\boldsymbol{\omega}}_{\mathcal{B}/\mathcal{N}} + [\tilde{\boldsymbol{\omega}}_{\mathcal{B}/\mathcal{N}}] [I_{\text{sc}, B}] \boldsymbol{\omega}_{\mathcal{B}/\mathcal{N}} + \sum_{i=1}^M \left(m_{\text{fuel}_i} [\tilde{\mathbf{r}}_{F_{c_i}/B}] \mathbf{r}''_{F_{c_i}/B} + \right. \\ &\left. + \dot{m}_{\text{fuel}_i} [\tilde{\mathbf{r}}_{F_{c_i}/B}] \mathbf{r}'_{F_{c_i}/B} + [I_{\text{fuel}_i, B}]' \boldsymbol{\omega}_{\mathcal{B}/\mathcal{N}} + m_{\text{fuel}_i} [\tilde{\boldsymbol{\omega}}_{\mathcal{B}/\mathcal{N}}] [\tilde{\mathbf{r}}_{F_{c_i}/B}] \mathbf{r}'_{F_{c_i}/B} \right) + \\ &+ \sum_{j=1}^N \int_{\dot{m}_{\text{noz}_j}} [\tilde{\mathbf{r}}_{M/B}]^T \mathbf{v}_{\text{exh}_j} d\dot{m} + \sum_{j=1}^N \int_{\dot{m}_{\text{noz}_j}} [\tilde{\mathbf{r}}_{M/B}] [\tilde{\mathbf{r}}_{M/B}] \boldsymbol{\omega}_{\mathcal{B}/\mathcal{N}} d\dot{m} + \\ &+ [\tilde{\mathbf{c}}] m_{\text{sc}} \ddot{\mathbf{r}}_{B/\mathcal{N}} = \mathbf{L}_{B, \text{vol}} + \mathbf{L}_{B, \text{surf}} \end{aligned} \quad (51)$$

The torque of each nozzle can be computed as a part given by the pressure distribution of exhausting flow and a second one provided by the lever arm distance from the application point of the force:

$$\mathbf{L}_{B_{\text{thr}_j}} = \mathbf{L}_{B_{\text{sc, noz}_j}} + \int_{\dot{m}_{\text{noz}_j}} \mathbf{r}_{M/B} \times \mathbf{v}_{\text{noz}_j} d\dot{m} \quad (52)$$

Furthermore, a term taking into account the angular momentum variation caused by mass depletion can be defined as follows:

$$[K] = \sum_{i=1}^M [I_{\text{fuel}_i, B}]' + \sum_{j=1}^N \int_{\dot{m}_{\text{noz}_j}} [\tilde{\mathbf{r}}_{M/B}] [\tilde{\mathbf{r}}_{M/B}] d\dot{m} \quad (53)$$

The second integral in equation 53 can be computed evaluating the momentum exchanged due to the fuel thin disc going out from the nozzle area, coincident in this case with part of the interface surface between the spacecraft and the exhausted fuel. If a series of N nozzles are considered, the integral can be split:

$$\begin{aligned} & \int_{\dot{m}_{\text{noz}_j}} [\tilde{\mathbf{r}}_{M/B}] [\tilde{\mathbf{r}}_{M/B}] d\dot{m} = \\ & = \int_{\dot{m}_{\text{noz}_j}} (([\tilde{\mathbf{r}}_{N_j/B}] + [\tilde{\mathbf{r}}_{M/N_j}]) ([\tilde{\mathbf{r}}_{N_j/B}] + [\tilde{\mathbf{r}}_{M/N_j}])) d\dot{m} = \\ & = -\dot{m}_{\text{noz}_j} \left([\tilde{\mathbf{r}}_{N_j/B}] [\tilde{\mathbf{r}}_{N_j/B}]^T + \frac{A_{\text{noz}_j}}{4\pi} [BM_j] \begin{bmatrix} 2 & 0 & 0 \\ 0 & 1 & 0 \\ 0 & 0 & 1 \end{bmatrix} [BM_j]^T \right) \quad (54) \end{aligned}$$

where A_{noz_j} is the exiting area of the j -th nozzle and $[BM_j]$ is the change coordinate matrix from the j -th nozzle frame \mathcal{M}_j , defined to have its origin in the N_j point and its first axis in the exhausting velocity direction $\mathbf{v}_{\text{exh}_j}$, to the B frame.

Finally the rotational equation of motion can be written:

$$\begin{aligned} & [I_{\text{sc}, B}] \dot{\boldsymbol{\omega}}_{\mathcal{B}/\mathcal{N}} + [\tilde{\boldsymbol{\omega}}_{\mathcal{B}/\mathcal{N}}] [I_{\text{sc}, B}] \boldsymbol{\omega}_{\mathcal{B}/\mathcal{N}} + \sum_{i=1}^M \left(m_{\text{fuel}_i} [\tilde{\mathbf{r}}_{F_{c_i}/B}] \mathbf{r}_{F_{c_i}/B}'' + \right. \\ & \quad \left. + \dot{m}_{\text{fuel}_i} [\tilde{\mathbf{r}}_{F_{c_i}/B}] \mathbf{r}_{F_{c_i}/B}' + m_{\text{fuel}_i} [\tilde{\boldsymbol{\omega}}_{\mathcal{B}/\mathcal{N}}] [\tilde{\mathbf{r}}_{F_{c_i}/B}] \mathbf{r}_{F_{c_i}/B}' \right) + \\ & \quad + K \boldsymbol{\omega}_{\mathcal{B}/\mathcal{N}} + [\tilde{\mathbf{c}}] m_{\text{sc}} \ddot{\mathbf{r}}_{B/\mathcal{N}} = \mathbf{L}_{B, \text{vol}} + \mathbf{L}_{B, \text{surf}} + \sum_{j=1}^N \mathbf{L}_{B_{\text{thr}_j}} \quad (55) \end{aligned}$$

4.2.1 The $[K]$ term

In this paragraph a brief dissertation about the $[K]$ matrix defined in equation 53 will be developed.

This matrix summarizes the angular momentum variation induced by the mass depletion. It is a symmetric matrix as it is the sum of matrices of this type and, as shown in equation 53, it depends directly from the nozzles' position and geometry and from the tanks' mass variation and their geometry.

In figure 3 a simple but instructive case is shown and it could be useful to clarify the influence of the $[K]$ term and can be analyzed in details in [7] where various tank configurations are considered and a dissertation of the spin and transversal rate is developed to understand the influence of the mass depletion on the system.

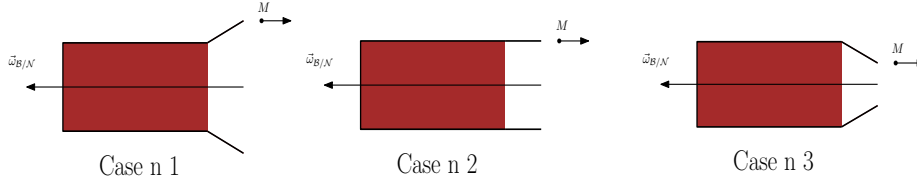


Figure 3: Cases of the influence of the $[K]$ matrix on the system dynamics.

In all the three cases a cylindrical tank is rotating about its symmetry axis \hat{e}_3 with constant angular velocity $\boldsymbol{\omega}_{B/N} = [0 \ 0 \ \omega_{B/N_z}]^T$ and, at a given time, it starts losing mass according to the force to be applied. On one hand, the angular momentum transported by a particle at the tank's wall will be:

$$\mathbf{H}_{\text{part, tank}} = m_{\text{part}} \mathbf{R}_{\text{tank}} \times (\mathbf{R}_{\text{tank}} \times \boldsymbol{\omega}_{B/N}) = m_{\text{part}} \begin{bmatrix} 0 \\ 0 \\ R_{\text{tank}}^2 \omega_{B/N_z} \end{bmatrix} \quad (56)$$

where m_{part} is the particle mass and \mathbf{R}_{tank} is the cylinder radius. On the other, the angular momentum of the same particle at the nozzle's exit can be easily written as follows:

$$\mathbf{H}_{\text{part, noz}} = m_{\text{part}} \mathbf{R}_{\text{noz}} \times (\mathbf{R}_{\text{noz}} \times \boldsymbol{\omega}_{B/N} + \mathbf{v}_{\text{exh}}) = m_{\text{part}} \begin{bmatrix} 0 \\ 0 \\ R_{\text{noz}}^2 \omega_{B/N_z} \end{bmatrix} \quad (57)$$

where \mathbf{R}_{noz} is the nozzle radius.

Obviously the angular momentum variation is equal to the amount of it transported throughout the surface control by the particles. Intuitively, three different cases can be distinguished:

1. If $R_{\text{tank}} < R_{\text{noz}}$, the particle is transporting out more angular momentum than the one it owned inside the tank as the distance from the symmetry axis \hat{e}_3 is bigger. As a consequence, the body tends to spin down and asymptotically stabilize the motion.

2. If $R_{\text{tank}} = R_{\text{noz}}$, the same amount of angular momentum possessed by the particle inside the tank is ejected from the nozzle and, consequently, the body does not modify its state of motion.
3. If $R_{\text{tank}} > R_{\text{noz}}$, the angular momentum difference is smaller than zero and the system spins up to compensate this gap.

5 Fuel supply architecture and implementation

From a program implementation prospective the tank mass flow and their derivatives must be computed once a maneuver is performed in order to evaluate the different terms in the equations of motion. By using this approach the j -th nozzle mass flow will be considered as known and could be computed from the thrust provided by the nozzle and its properties, i.e. I_{sp_j} and $\mathbf{v}_{\text{noz}_j}$. If a matrix notation is considered:

$$\dot{\mathbf{m}}_{\text{fuel}} = [A] \dot{\mathbf{m}}_{\text{noz}} \quad (58)$$

where $[A]$ is a matrix linking the tanks' mass flows and nozzles' ones. A fundamental property of the matrix A can be established from the definition of $\dot{\mathbf{m}}_{\text{fuel}}$:

$$\sum_{i=1}^M \dot{m}_{\text{fuel}_i} = \sum_{i=1}^M \sum_{j=1}^N A_{ij} \dot{m}_{\text{noz}_j} = \sum_{j=1}^N \dot{m}_{\text{noz}_j} \Rightarrow \sum_{i=0}^M A_{ij} = 1 \quad \forall j \in (1, N) \quad (59)$$

The previous property is a direct consequence of the mass flow conservation between the tanks and the nozzles.

From the previous relation, the first derivative of mass flows can be easily computed:

$$\ddot{\mathbf{m}}_{\text{fuel}} = [A] \ddot{\mathbf{m}}_{\text{noz}} + [\dot{A}] \dot{\mathbf{m}}_{\text{noz}} \quad (60)$$

In the following analysis the $[A]$ will be considered constant with time, i.e. $[\dot{A}] = 0$. In figure 4 an example of a possible distribution system is shown.

Taking into account this schematic representation and the fact that each component of the matrix $[A]_{ij}$ represent the percentage of fuel ejected by the nozzle j given from the tank i , an example can be easily developed. The system of equation is:

$$\begin{cases} \dot{m}_{\text{fuel}_1} = \dot{m}_{\text{noz}_1} + \dot{m}_{\text{noz}_2} \\ \dot{m}_{\text{fuel}_2} = 0.3 \dot{m}_{\text{noz}_4} + \dot{m}_{\text{noz}_5} \\ \dot{m}_{\text{fuel}_3} = \dot{m}_{\text{noz}_3} + 0.7 \dot{m}_{\text{noz}_4} \end{cases} \quad (61)$$

Thus, the $[A]$ matrix is:

$$[A] = \begin{bmatrix} 1 & 1 & 0 & 0 & 0 \\ 0 & 0 & 0 & 0.3 & 1 \\ 0 & 0 & 1 & 0.7 & 0 \end{bmatrix} \quad (62)$$

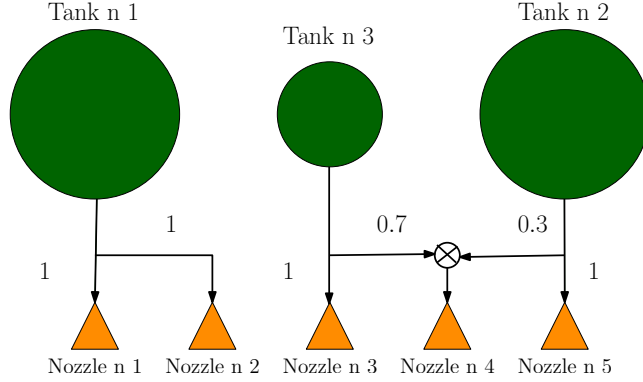


Figure 4: An example of the distribution system among tanks and nozzles with numerical values.

6 Control feedback law

Once equations have been gathered, control can be included to reach the desired reference state despite the disturbances applied on the spacecraft.

According to reference [8], a Modified Rodrigues Parameters (MRP) feedback control law has been chosen as it can always assure global asymptotic stability avoiding singularities. If a reference frame \mathcal{R} is defined, the control can be expressed as follows:

$$\mathbf{u} = -K \boldsymbol{\sigma}_{\mathcal{B}/\mathcal{R}} - P \boldsymbol{\omega}_{\mathcal{B}/\mathcal{R}} \quad (63)$$

where $\boldsymbol{\sigma}_{\mathcal{B}/\mathcal{R}}$ is the MRP defining the attitude from the \mathcal{R} frame to the \mathcal{B} one and $\boldsymbol{\omega}_{\mathcal{B}/\mathcal{R}}$ is the angular velocity of the \mathcal{B} frame about the \mathcal{R} one. The importance of using a \mathcal{R} frame instead the inertial one \mathcal{N} lies in the possibility of moving the reference frame about the latter to let the spacecraft orient its axis as desired in the euclidean space imposing both the attitude and the angular velocity. A clear example of this concept could be a reference frame \mathcal{R} spinning about the inertial frame \mathcal{N} .

In order to evaluate the control torque the attitude $\boldsymbol{\sigma}_{\mathcal{B}/\mathcal{R}}$ and the angular velocity $\boldsymbol{\omega}_{\mathcal{B}/\mathcal{R}}$ must be computed. By considering as known $\boldsymbol{\sigma}_{\mathcal{R}/\mathcal{N}}$ and $\boldsymbol{\omega}_{\mathcal{R}/\mathcal{N}}$, the needed variables can be calculated as follows [8, 9]:

$$\begin{aligned} \boldsymbol{\sigma}_{\mathcal{B}/\mathcal{R}} &= \boldsymbol{\sigma}_{\mathcal{B}/\mathcal{N}} \odot \boldsymbol{\sigma}_{\mathcal{R}/\mathcal{N}} = \\ &= \frac{\left(1 - \boldsymbol{\sigma}_{\mathcal{B}/\mathcal{N}}^T \boldsymbol{\sigma}_{\mathcal{B}/\mathcal{N}}\right) \boldsymbol{\sigma}_{\mathcal{R}/\mathcal{N}} + \left(1 - \boldsymbol{\sigma}_{\mathcal{R}/\mathcal{N}}^T \boldsymbol{\sigma}_{\mathcal{R}/\mathcal{N}}\right) \boldsymbol{\sigma}_{\mathcal{B}/\mathcal{N}} - 2 \boldsymbol{\sigma}_{\mathcal{R}/\mathcal{N}} \times \boldsymbol{\sigma}_{\mathcal{B}/\mathcal{N}}}{1 + \left(\boldsymbol{\sigma}_{\mathcal{B}/\mathcal{N}}^T \boldsymbol{\sigma}_{\mathcal{B}/\mathcal{N}}\right) \left(\boldsymbol{\sigma}_{\mathcal{R}/\mathcal{N}}^T \boldsymbol{\sigma}_{\mathcal{R}/\mathcal{N}}\right) + 2 \boldsymbol{\sigma}_{\mathcal{B}/\mathcal{N}}^T \boldsymbol{\sigma}_{\mathcal{R}/\mathcal{N}}} \end{aligned} \quad (64)$$

$$\boldsymbol{\omega}_{\mathcal{B}/\mathcal{R}} = \boldsymbol{\omega}_{\mathcal{B}/\mathcal{N}} - \boldsymbol{\omega}_{\mathcal{R}/\mathcal{N}} \quad (65)$$

where, in case of singular representation of the MRP set $\boldsymbol{\sigma}_{\mathcal{B}/\mathcal{R}}$, one of the two initial MRP can be switched to the shadow representation ${}^S\boldsymbol{\sigma}_{\mathcal{B}/\mathcal{N}}$ defined by:

$${}^S\boldsymbol{\sigma} = -\frac{\boldsymbol{\sigma}}{\boldsymbol{\sigma}^T \boldsymbol{\sigma}} \quad (66)$$

For a detailed treatment and the kinematic relations among the different angular representations, the references [8] could be used.

The control torque might be concretely provided to the spacecraft through various devices and, in the present paper, a thruster-based control will be implemented to underline the main features of mass depletion.

The challenge of this approach is to find out the needed forces from a given torque. The following algorithm has been provided by Dr. Hanspeter Schaub and has not been developed by the author.

By assuming a series of P ACS thrusters, the position of the k -th nozzle can be labeled $\mathbf{r}_{N_k/B}$ and the k -th force is given by:

$$\mathbf{F}_{\text{thr}_k} = F_{\text{thr}_k} \hat{\mathbf{g}}_k = F_{\text{thr}_k} [BM_k] \hat{\mathbf{m}}_1 \quad (67)$$

where $\hat{\mathbf{m}}_1$ is the first versor of the k -th ADC thruster's reference frame as defined previously. Consequently, the torque generated can be easily computed:

$$\mathbf{L}_{B_{\text{thr}_k}} = \mathbf{r}_{N_k/B} \times F_{\text{thr}_k} \hat{\mathbf{g}}_k \quad (68)$$

If a set of ortho-normal, i.e. $\hat{\mathbf{c}}_h \cdot \hat{\mathbf{c}}_h = 1$ and $\hat{\mathbf{c}}_h \cdot \hat{\mathbf{c}}_r$ for $r, h \in (1, 3)$, axis is chosen the total torque provided by the thrusters about the $\hat{\mathbf{c}}_h$ is:

$$\mathbf{L}_{B_{\text{thr}}} \cdot \hat{\mathbf{c}}_h = \sum_{k=1}^P \mathbf{L}_{B_{\text{thr}_k}} \cdot \hat{\mathbf{c}}_h = \sum_{k=1}^P (\mathbf{r}_{N_k/B} \times \hat{\mathbf{g}}_k) \cdot \hat{\mathbf{c}}_h F_{\text{thr}_k} = \sum_{k=1}^P d_k F_{\text{thr}_k} \quad (69)$$

In a matrix form:

$$\mathbf{L}_{B_{\text{thr}}} \cdot \hat{\mathbf{c}}_h = [D] \mathbf{F}_{\text{thr}} \quad (70)$$

The first step to compute the forces is to find which thrusters could provide positive F_{thr_k} , thus in accord with the definition of F_{thr_k} as magnitude of the force vector. This can be actually achieved by a minimum norm solution to produce the needed control torque:

$$\mathbf{F}_{\text{thr}} = [D]^T \left([D] [D]^T \right)^{-1} \mathbf{u} \cdot \hat{\mathbf{c}}_h \quad (71)$$

By considering the \bar{P} thrusters providing positive magnitude from Equation 71 and calling $\bar{\mathbf{F}}_{\text{thr}}$ the vector containing their magnitude, $[D]$ is a $3 \times \bar{P}$ matrix defined as follows:

$$\bar{\mathbf{d}}_k = \mathbf{r}_{N_k/B} \times \hat{\mathbf{g}}_k \quad (72)$$

From this definition, the thruster mapping is:

$$[D] \bar{\mathbf{F}}_{\text{thr}} = \hat{\mathbf{c}}_h (\mathbf{u} \cdot \hat{\mathbf{c}}_h) \quad (73)$$

At the same time, the thruster should not produce a net force on the spacecraft in order not to influence the translational motion. Thus:

$$\overline{\mathbf{F}} = [\overline{G}] \overline{\mathbf{F}}_{\text{thr}} = 0 \quad (74)$$

where $[\overline{G}]$ is a $3 \times \overline{P}$ matrix containing the thrust's direction.

In order to minimize the net force applied on the spacecraft with the constrains of obtaining a given torque, the following functional must be minimized:

$$J = \frac{1}{2} \overline{\mathbf{F}}_{\text{thr}}^T [\overline{G}]^T [\overline{G}] \overline{\mathbf{F}}_{\text{thr}} + \boldsymbol{\lambda}^T ([\overline{D}] \overline{\mathbf{F}}_{\text{thr}} - \hat{\mathbf{c}}_h (\mathbf{u} \cdot \hat{\mathbf{c}}_h)) \quad (75)$$

where $\boldsymbol{\lambda}$ is the 3×1 Lagrange multiplier vector. By imposing its gradient equals to zero, the set of forces provided by the chosen nozzles can be computed.

$$\begin{bmatrix} \overline{G}^T \overline{G} & \overline{D}^T \\ \overline{D} & \mathbf{0}_{3 \times 3} \end{bmatrix} \begin{bmatrix} \mathbf{F}_{\text{thr}} \\ \boldsymbol{\lambda} \end{bmatrix} = \begin{bmatrix} \mathbf{0}_{\overline{P} \times 1} \\ \hat{\mathbf{c}}_h (\mathbf{u} \cdot \hat{\mathbf{c}}_h) \end{bmatrix} \quad (76)$$

This procedure is applied for every component of the control \mathbf{u} and, finally, the net force generated can be computed summing the force generated from the P nozzle:

$$\mathbf{F}_{\text{net}} = \sum_{k=1}^P \mathbf{F}_{\text{thr}_k} \quad (77)$$

It must be noticed that this approach does not require a symmetric ADC thrusters' configuration and can be applied to whichever set of thruster minimizing the net force and providing the needed control torque.

7 Tank models

Different tank model could be developed to perfectly suit the needs of the spacecraft's fuel chain configuration. In the present paper five reservoir model will be considered as examples and their properties such as inertia variation and barycenter motion will be gathered.

The models and the main hypothesis are presented below:

- The constant tank's volume model where a spherical reservoir maintains a fixed geometry, i.e. a constant radius, and a fixed barycenter.
- The constant fuel's density model where a spherical tank keeps its geometrical shape but gradually change its volume, so its radius, to maintain the density of the fuel constant and it has a fixed center of mass.
- The emptying tank model where the fuel leaks out from an outlet in the spherical reservoir and the quantity of fuel decrease perpendicularly to the output direction modifying the barycenter position and the body's inertia accordingly to the mass distribution inside the tank.

- The uniform burn cylinder model where a cylindrical tanks does not change its geometrical shape and volume but the gas gradually decrease its density. As a consequence, the fuel barycenter remains fixed and the inertia varies accordingly to the mass variation.
- The centrifugal burn cylinder model where a cylindrical tank is considered and the fuel burns radially from the center to the walls without breaking the tank's symmetry. The inertia tensor derivative is computed from these hypothesis and the barycenter remains in its initial position as the symmetry is conserved.

7.1 The constant tank's volume model

This model takes into account the variation of the fuel inside the satellite considering no variation of the volume off the tank. By looking at Figure 5:

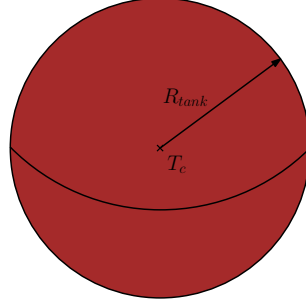


Figure 5: Geometrical properties of the constant density sphere.

$$V_{\text{tank}} = \text{cost} \quad \Rightarrow \quad R_{\text{tank}} = \text{cost} \quad (78)$$

$$[I_{\text{fuel}}, T_c] = \frac{2}{5} m_{\text{fuel}} R_{\text{tank}}^2 [\mathbb{1}_{3 \times 3}] \quad (79)$$

$$[I_{\text{fuel}}, T_c]' = \frac{2}{5} \dot{m}_{\text{fuel}} R_{\text{tank}}^2 [\mathbb{1}_{3 \times 3}] \quad (80)$$

Moreover the position of the center of mass of the tank does not change, so:

$$\mathbf{r}'_{T_c/B} = 0 \quad \mathbf{r}''_{T_c/B} = 0 \quad (81)$$

7.2 The constant fuel's density model

The second model considers a shape-changeable tank adapting itself to keep the fuel's density constant. Thus, according to Figure 6:

$$\begin{cases} \dot{V}_{\text{tank}} = \frac{\dot{m}_{\text{fuel}}}{\rho_{\text{fuel}}} \\ \dot{V}_{\text{tank}} = 4\pi R_{\text{tank}}^2 \dot{R}_{\text{tank}} \end{cases} \quad \Rightarrow \quad \dot{R}_{\text{tank}} = \frac{\dot{m}_{\text{fuel}}}{4\pi R_{\text{tank}}^2 \rho_{\text{fuel}}} \quad (82)$$

As a consequence:

$$[I_{\text{fuel}}, T_c] = \frac{2}{5} m_{\text{fuel}} R_{\text{tank}}^2 [\mathbb{1}_{3 \times 3}] \quad (83)$$

$$\begin{aligned} [I_{\text{fuel}}, T_c]' &= \frac{2}{5} \left(R_{\text{tank}}^2 + \frac{m_{\text{fuel}}}{2\pi R_{\text{tank}} \rho_{\text{fuel}}} \right) \dot{m}_{\text{fuel}} [\mathbb{1}_{3 \times 3}] = \\ &= \frac{2}{5} \left(R_{\text{tank}}^2 + \frac{2}{3} R_{\text{tank}}^2 \right) \dot{m}_{\text{fuel}} [\mathbb{1}_{3 \times 3}] = \frac{2}{3} \dot{m}_{\text{fuel}} R_{\text{tank}}^2 [\mathbb{1}_{3 \times 3}] \end{aligned} \quad (84)$$

As in the previous model:

$$\mathbf{r}'_{T_c/B} = 0 \quad \mathbf{r}''_{T_c/B} = 0 \quad (85)$$

7.3 The emptying tank model

In this case the mass variation starts from the opposite point to the outlet, that will be called from now on the pole, perpendicularly to the vector connecting the pole and the outlet.

The following notation will be used: $\theta \in (0, \pi)$ will be the latitude angle counted from the pole till the outlet, $\phi \in (0, 2\pi)$ will note the longitude angle, the radius will be $r \in (0, R_{\text{tank}})$. Moreover the θ^* will denote the angle between the pole and the circumference of the fuel's free surface. The volume \mathcal{V} and the center of mass of the tank can be computed using notations in figure 7:

$$\begin{aligned} \mathcal{V}(\theta^*) &= \int_0^{2\pi} \int_0^{\theta^*} \int_0^{R_{\text{tank}} \frac{\cos \theta^*}{\cos \theta}} r^2 \sin \theta \, d\theta \, d\phi \, dr + \\ &+ \int_0^{2\pi} \int_{\theta^*}^{\pi} \int_0^{R_{\text{tank}}} r^2 \sin \theta \, d\theta \, d\phi \, dr = \frac{2\pi R_{\text{tank}}^3}{3} \left[1 + \frac{3}{2} \cos \theta^* - \frac{1}{2} \cos^3 \theta^* \right] \end{aligned} \quad (86)$$

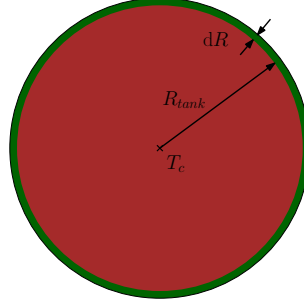


Figure 6: Geometrical properties of the constant density sphere.

$$\begin{aligned}
\mathbf{r}_{Tc/B} \cdot \hat{\mathbf{k}}_3 &= \mathbf{r}_{Tc'/B} \cdot \hat{\mathbf{k}}_3 + \frac{1}{\mathcal{V}(\theta^*)} \left(\int_0^{2\pi} \int_0^{\theta^*} \int_0^{R_{\text{tank}} \frac{\cos \theta^*}{\cos \theta}} r^3 \sin \theta \cos \theta \, d\theta \, d\phi \, dr + \right. \\
&+ \left. \int_0^{2\pi} \int_{\theta^*}^{\pi} \int_0^{R_{\text{tank}}} r^3 \sin \theta \cos \theta \, d\theta \, d\phi \, dr \right) = \frac{\pi R_{\text{tank}}^4}{4\mathcal{V}(\theta^*)} [2 \cos^2 \theta^* - \cos^4 \theta^* - 1]
\end{aligned} \tag{87}$$

where $\hat{\mathbf{k}}_3$ is the outlet-to-pole axis of the reference frame of the sphere and $\mathbf{r}_{Tc'/B}$ the constant vector from B to the center of the sphere. Considering that $m_{\text{fuel}} = \rho_{\text{fuel}} \mathcal{V}$, the derivatives in the \mathcal{B} reference frame can be performed:

$$\begin{aligned}
\mathbf{r}'_{Tc/B} \cdot \hat{\mathbf{k}}_3 &= -\frac{\pi R_{\text{tank}}^4 \rho_{\text{fuel}}}{4 m_{\text{fuel}}^2} \left[4 m_{\text{fuel}} \dot{\theta}^* \sin^3 \theta^* \cos \theta^* + \right. \\
&\quad \left. + \dot{m}_{\text{fuel}} (2 \cos^2 \theta^* - \cos^4 \theta^* - 1) \right] \tag{88}
\end{aligned}$$

$$\begin{aligned}
\mathbf{r}''_{Tc/B} \cdot \hat{\mathbf{k}}_3 &= -\frac{\pi R_{\text{tank}}^4 \rho_{\text{fuel}}}{2 m_{\text{fuel}}^3} \left[4 m_{\text{fuel}} \sin^3 \theta^* \cos \theta^* (\ddot{\theta}^* m_{\text{fuel}} - 2 \dot{\theta}^* \dot{m}_{\text{fuel}}) + \right. \\
&\quad - 4 m_{\text{fuel}}^2 \dot{\theta}^{*2} \sin^2 \theta^* (3 \cos^2 \theta^* - \sin^2 \theta^*) + \\
&\quad \left. + (2 \cos^2 \theta^* - \cos^4 \theta^* - 1) (m_{\text{fuel}} \ddot{m}_{\text{fuel}} - 2 \dot{m}_{\text{fuel}}^2) \right] \tag{89}
\end{aligned}$$

The relation among \dot{m}_{fuel} , \ddot{m}_{fuel} , $\dot{\theta}^*$ and $\ddot{\theta}^*$ is gathered from the derivation of the relation between the volume \mathcal{V} and m_{fuel} :

$$\begin{aligned}
m_{\text{fuel}} = \rho_{\text{fuel}} \mathcal{V}(\theta^*) &\Rightarrow \dot{m}_{\text{fuel}} = \rho_{\text{fuel}} \dot{\mathcal{V}}(\theta^*) \\
\dot{m}_{\text{fuel}} &= -\pi \rho_{\text{fuel}} R_{\text{tank}}^3 \sin^3 \theta^* \dot{\theta}^* \tag{90}
\end{aligned}$$

$$\ddot{m}_{\text{fuel}} = -\pi \rho_{\text{fuel}} R_{\text{tank}}^3 \sin^2 \theta^* (\ddot{\theta}^* \sin \theta^* + 3 \dot{\theta}^{*2} \cos \theta^*) \tag{91}$$

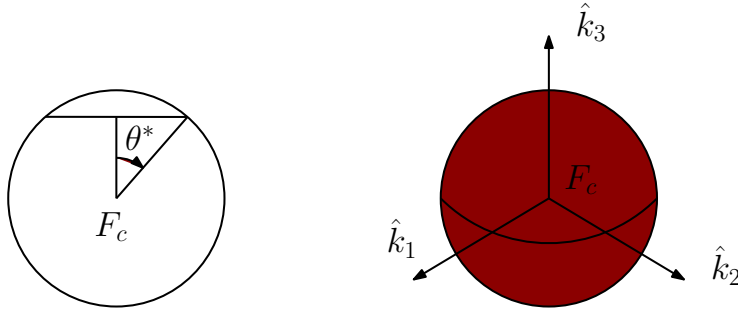


Figure 7: Geometrical properties of the emptying tank model.

Finally θ^* can be found:

$$m_{\text{fuel}} = \rho_{\text{fuel}} \mathcal{V}(\theta^*) \Rightarrow m_{\text{fuel}} = \frac{2}{3} \pi \rho_{\text{fuel}} R_{\text{tank}}^3 \left[1 + \frac{3}{2} \cos \theta^* - \frac{1}{2} \cos^3 \theta^* \right] \quad (92)$$

As far as the inertia concerns:

$$\begin{aligned} I_{33} &= \rho_{\text{fuel}} \left(\int_0^{2\pi} \int_0^{\theta^*} \int_0^{R_{\text{tank}} \frac{\cos \theta^*}{\cos \theta}} r^4 \sin^3 \theta \, d\theta \, d\phi \, dr + \right. \\ &\quad \left. + \int_0^{2\pi} \int_{\theta^*}^{\pi} \int_0^{R_{\text{tank}}} r^4 \sin^3 \theta \, d\theta \, d\phi \, dr \right) = \\ &= \frac{2}{5} \pi \rho_{\text{fuel}} R_{\text{tank}}^5 \left[\frac{2}{5} + \frac{1}{4} \cos \theta^* \sin^4 \theta^* - \frac{1}{12} (\cos 3\theta^* - 9 \cos \theta^*) \right] \quad (93) \end{aligned}$$

$$\begin{aligned} I_{22} &= \rho_{\text{fuel}} \left(\int_0^{2\pi} \int_0^{\theta^*} \int_0^{R_{\text{tank}} \frac{\cos \theta^*}{\cos \theta}} r^4 (\sin \theta - \sin^3 \theta \sin^2 \phi) \, d\theta \, d\phi \, dr + \right. \\ &\quad \left. + \int_0^{2\pi} \int_{\theta^*}^{\pi} \int_0^{R_{\text{tank}}} r^4 (\sin \theta - \sin^3 \theta \sin^2 \phi) \, d\theta \, d\phi \, dr \right) = \frac{2}{5} \pi \rho_{\text{fuel}} R_{\text{tank}}^5 \left[\frac{2}{3} + \right. \\ &\quad \left. - \frac{1}{4} \cos^5 \theta^* + \frac{1}{24} (\cos 3\theta^* - 9 \cos \theta^*) + \frac{5}{4} \cos \theta^* + \frac{1}{8} \cos \theta^* \sin^4 \theta^* \right] \quad (94) \end{aligned}$$

$$\begin{aligned} I_{11} &= \rho_{\text{fuel}} \left(\int_0^{2\pi} \int_0^{\theta^*} \int_0^{R_{\text{tank}} \frac{\cos \theta^*}{\cos \theta}} r^4 (\sin \theta - \sin^3 \theta \cos^2 \phi) \, d\theta \, d\phi \, dr + \right. \\ &\quad \left. + \int_0^{2\pi} \int_{\theta^*}^{\pi} \int_0^{R_{\text{tank}}} r^4 (\sin \theta - \sin^3 \theta \cos^2 \phi) \, d\theta \, d\phi \, dr \right) = I_{22} \quad (95) \end{aligned}$$

$$\begin{aligned} I_{12} &= \rho_{\text{fuel}} \left(\int_0^{2\pi} \int_0^{\theta^*} \int_0^{R_{\text{tank}} \frac{\cos \theta^*}{\cos \theta}} r^4 \sin^3 \theta \cos \phi \sin \phi \, d\theta \, d\phi \, dr + \right. \\ &\quad \left. + \int_0^{2\pi} \int_{\theta^*}^{\pi} \int_0^{R_{\text{tank}}} r^4 \sin^3 \theta \cos \phi \sin \phi \, d\theta \, d\phi \, dr \right) = 0 \quad (96) \end{aligned}$$

$$\begin{aligned} I_{13} &= \rho_{\text{fuel}} \left(\int_0^{2\pi} \int_0^{\theta^*} \int_0^{R_{\text{tank}} \frac{\cos \theta^*}{\cos \theta}} r^4 \sin^2 \theta \cos \theta \cos \phi \, d\theta \, d\phi \, dr + \right. \\ &\quad \left. + \int_0^{2\pi} \int_{\theta^*}^{\pi} \int_0^{R_{\text{tank}}} r^4 \sin^2 \theta \cos \theta \cos \phi \, d\theta \, d\phi \, dr \right) = 0 \quad (97) \end{aligned}$$

$$I_{23} = \rho_{\text{fuel}} \int_0^{2\pi} \int_0^{\theta^*} \int_0^{R_{\text{tank}} \frac{\cos \theta^*}{\cos \theta}} r^4 \sin^2 \theta \cos \theta \sin \phi \, d\theta \, d\phi \, dr = 0 \quad (98)$$

because $\int_0^{2\pi} \cos \phi \sin \phi \, d\phi = \int_0^{2\pi} \sin \phi \, d\phi = \int_0^{2\pi} \cos \phi \, d\phi = 0$.

From those calculations the derivatives, in the tank reference frame, can be computed:

$$I'_{33} = \frac{2}{5} \pi \rho_{\text{fuel}} R_{\text{tank}}^5 \dot{\theta}^* \left[\cos^2 \theta^* \sin^3 \theta^* - \frac{1}{4} \sin^5 \theta^* + \frac{1}{4} \sin 3\theta^* - \frac{3}{4} \sin \theta^* \right] \quad (99)$$

$$I'_{22} = I'_{11} = \frac{2}{5} \pi \rho_{\text{fuel}} R_{\text{tank}}^5 \dot{\theta}^* \left[\frac{5}{4} \sin \theta^* \cos \theta^* - \frac{5}{4} \sin \theta^* - \frac{1}{8} \sin 3\theta^* + \frac{3}{8} \sin \theta^* + \frac{1}{2} \cos^2 \theta^* \sin^3 \theta^* - \frac{1}{8} \sin^5 \theta^* \right] \quad (100)$$

7.4 Uniform burn cylinder

This model consider a cylindrical tank whose geometry remains constant while fuel density changes. From these considerations and by looking at Figure 8, the

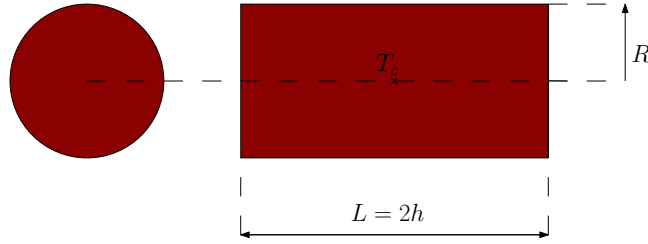


Figure 8: Geometrical properties of the uniform burn cylinder

inertia tensor and it's derivative could be evaluated:

$$I_{11} = I_{22} = m_{\text{fuel}} \left[\frac{R^2}{4} + \frac{h^2}{3} \right] \quad I_{33} = m_{\text{fuel}} \frac{R^2}{2} \quad (101)$$

$$I'_{11} = I'_{22} = \dot{m}_{\text{fuel}} \left[\frac{R^2}{4} + \frac{h^2}{3} \right] \quad I'_{33} = \dot{m}_{\text{fuel}} \frac{R^2}{2} \quad (102)$$

where R is the cylinder radius and h its half-height.

Moreover, as the position of the center of mass of the tank does not change:

$$\mathbf{r}'_{Tc/B} = 0 \quad \mathbf{r}''_{Tc/B} = 0 \quad (103)$$

7.5 Centrifugal burn cylinder

The present model consider a cylinder filled with propellant burning radially from the center to the edge. The geometry properties and their nomenclature can be seen in Figure 9.

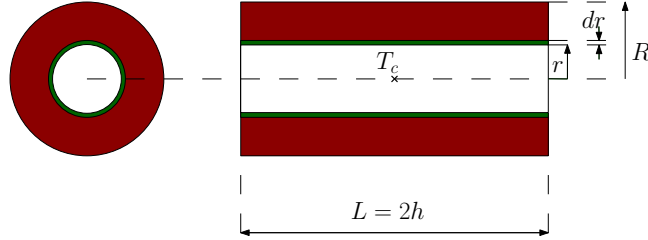


Figure 9: Geometrical properties of the centrifugal burn cylinder

By denoting r the distance of the fuel surface from the axis of the cylinder, this quantity can be easily computed from the amount of mass in the tank:

$$r = \sqrt{R^2 - \frac{m_{\text{fuel}}}{2\pi\rho h}} \quad (104)$$

where R is the cylinder radius, h its half-height and ρ the fuel density. As in the previous models, the time derivative of r can be gathered from volume-mass relation:

$$\dot{m}_{\text{fuel}} = -4\pi\rho h r \dot{r} \quad (105)$$

As a consequence:

$$I_{11} = I_{22} = m_{\text{fuel}} \left[\frac{R^2 + r^2}{4} + \frac{h^2}{3} \right] \quad (106)$$

$$I_{33} = m_{\text{fuel}} \left[\frac{R^2 + r^2}{2} \right] \quad (107)$$

Moreover, their time derivative in the tank's reference frame can be computed:

$$I'_{11} = I'_{22} = \dot{m}_{\text{fuel}} \left[\frac{r^2}{2} + \frac{h^2}{3} \right] \quad (108)$$

$$I'_{33} = \dot{m}_{\text{fuel}} r^2 \quad (109)$$

Finally, the tank's center of mass does not change as the mass variation is symmetric. Thus:

$$\mathbf{r}'_{T_c/B} = 0 \quad \mathbf{r}''_{T_c/B} = 0 \quad (110)$$

8 Thruster models

The present section presents the thruster's model developed and used in the present paper.

Some general properties of the thruster are here summarized. Firstly, the thrust will be assumed to follow the specific impulse relation expressed in Equation 27. As a consequence, the impulse, and thus the velocity variation, can be easily computed:

$$\Delta \mathbf{v} = I_{\text{sp}} g_0 \frac{\mathbf{v}_{\text{exh}}}{v_{\text{exh}}} \int_{m_{\text{in}}}^{m_{\text{fin}}} \frac{dm}{m} = I_{\text{sp}} g_0 \frac{\mathbf{v}_{\text{exh}}}{v_{\text{exh}}} \ln \left(\frac{m_{\text{fin}}}{m_{\text{in}}} \right) \quad (111)$$

where m_{in} is the initial mass of the spacecraft and m_{fin} is the final one. The equation is normally projected on the force axis to obtain the wide-known scalar equation:

$$\Delta v = I_{\text{sp}} g_0 \ln \left(\frac{m_{\text{in}}}{m_{\text{fin}}} \right) \quad (112)$$

It must be underlined that this equation is not dependent from the force law applied on the spacecraft as far as the specific impulse relation stands.

Two simple examples of thruster are presented briefly in the list below and then exposed in the following paragraphs.

- The impulsive thruster model where the thrust is immediately generated during the firing time.
- The ramping thruster model where, once the valve is opened to provide thrust, a time span of response Δt_{resp} is required to acquire the steady state.

It must be underlined that the modularity and adaptability of the code permit the use of complex models which could be implemented directly from the user.

8.1 Impulsive model

This section presents the simplest model developed to simulate the satellite attitude. The thrust has the following expression:

$$\mathbf{F}(t) = \begin{cases} I_{\text{sp}} g_0 \dot{m}_{\text{fuel}} \frac{\mathbf{v}_{\text{exh}}}{v_{\text{exh}}} & \text{if } t_{\text{in fir}} \leq t \leq t_{\text{fin fir}} \\ 0 & \text{otherwise} \end{cases} \quad (113)$$

where $t_{\text{in fir}}$ is the initial firing time and $t_{\text{fin fir}}$ is the final firing time.

The dynamical characteristics associated with this type of thruster are presented in Figures 10. The absence of \ddot{m}_{fuel} is a simplification of the singular derivative that could be obtained from the step function. This lead to a rapid and easier implementation without losing precious details during the simulation.

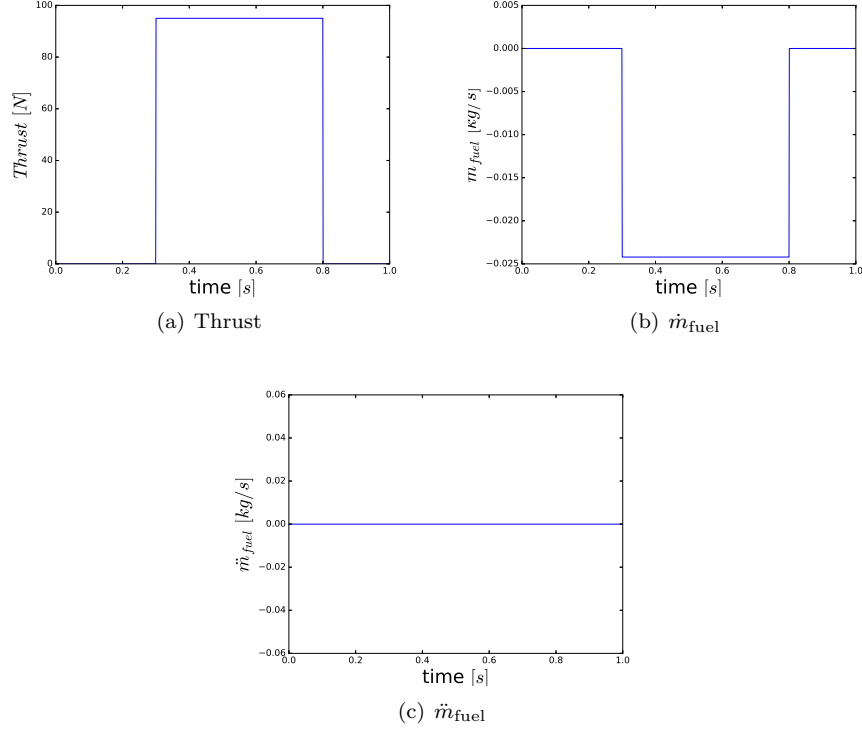


Figure 10: Characteristics of the impulsive thruster firing from $t = 0.3$ s to $t = 0.8$ s. In the shown simulation: $I_{sp} = 400$ s and $g_0 = 9.81 \frac{m}{s^2}$.

8.2 Ramping model

A more sophisticated approach is presented in this paragraph. The thruster model is not perfectly fitting reality as the continuity of the fuel rate derivative is not assured. Despite that, a first order approximation of the ramping up and down of the fuel rate can be evaluated without entering into details of a complex implementation. This model consider a time interval Δt_{resp} where the thruster's valve cannot provide the needed amount of fuel and, as a consequence, a straight line transient connects the zero state to the steady one. The mathematical expression of this model is:

$$F(t) = \begin{cases} I_{sp} g_0 \dot{m}_{fuel} \frac{v_{exh}}{v_{exh}} (t - t_{in_fir}) & \text{if } t_{in_fir} \leq t \leq t_{in_fir} + \Delta t_{resp} \\ I_{sp} g_0 \dot{m}_{fuel} \frac{v_{exh}}{v_{exh}} & \text{if } t_{in_fir} + \Delta t_{resp} < t \leq t_{fin_fir} \\ I_{sp} g_0 \dot{m}_{fuel} \frac{v_{exh}}{v_{exh}} (t_{fin_fir} + \Delta t_{resp} - t) & \text{if } t_{fin_fir} < t \leq t_{fin_fir} + \Delta t_{resp} \\ 0 & \text{otherwise} \end{cases} \quad (114)$$

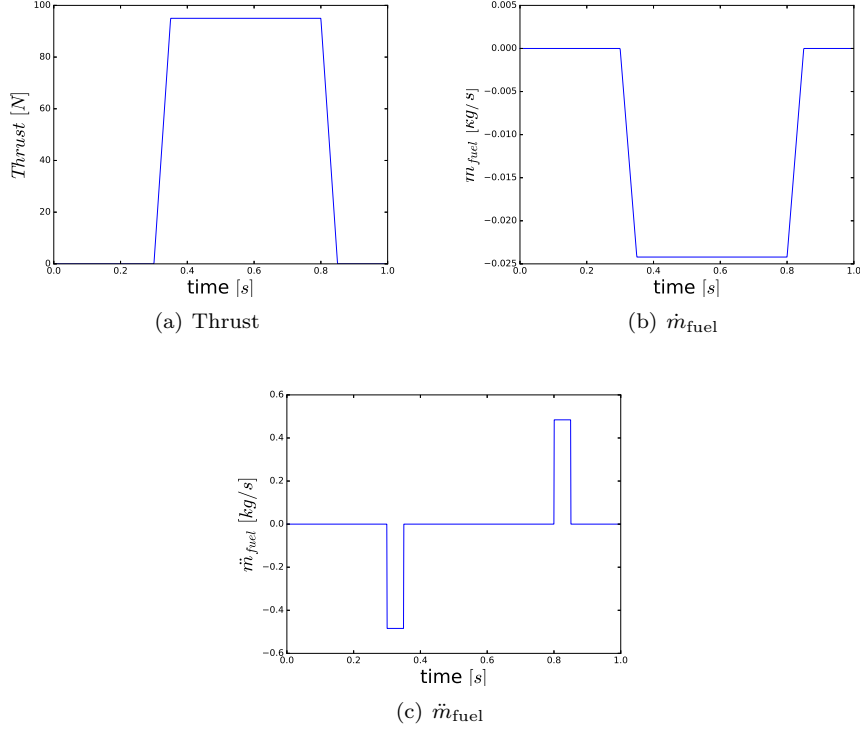


Figure 11: Characteristics of the ramping thruster firing from $t = 0.3 \text{ s}$ to $t = 0.8 \text{ s}$. In the shown simulation: $I_{\text{sp}} = 400 \text{ s}$, $g_0 = 9.81 \frac{\text{m}}{\text{s}^2}$ and $\Delta t_{\text{resp}} = 50 \text{ ms}$.

where Δt_{resp} has been previously defined. In Figures 11, the main properties of the thruster are presented for a 0.5 s firing interval.

9 Numerical Implementation

INSERIRE DIGITAL IMPEMENTATION

10 Results

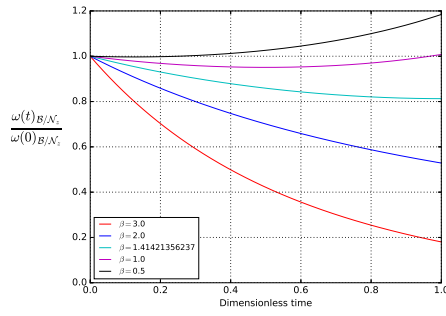
In the present section the results obtained by the developed method, implemented in a Python environment, for different cases.

Firstly validating simulation will be shown to provide a way to validate the present model, where neither the angular momentum nor the energy are constant, and successively a series of fuel demanding maneuver will be exposed in order to underline the importance to take into account the mass depletion for high-accuracy pointing, simulation and control law design.

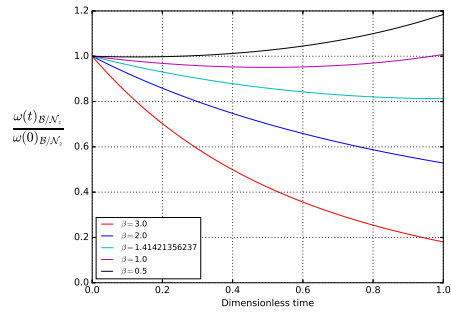
10.1 Axial-symmetric rocket

The following simulations have been performed to reproduce the results outlined in [7] and validate the developed model.

10.1.1 Centrifugal burn

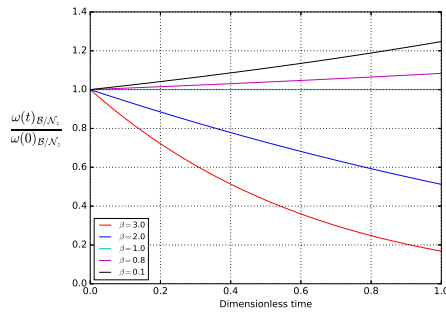


(a) Spin rate evolution in time

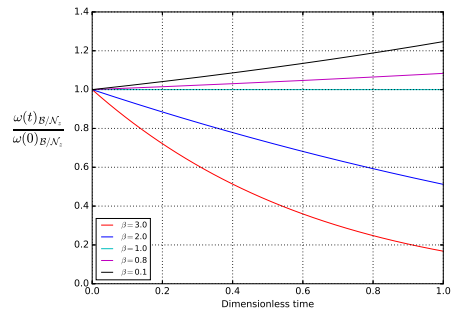


(b) Traversal rate evolution in time

10.1.2 Uniform burn



(c) Spin rate evolution in time



(d) Traversal rate evolution in time

10.2 De-tumbling maneuver

10.3 LEO-to-GEO maneuver

11 Conclusions

References

- [1] R. W. Fox, A. T. McDonald, and P. J. Pritchard, *Introduction to fluid mechanics*, Vol. 7. John Wiley & Sons New York, 1985.
- [2] F. White, *Fluid Mechanics*. McGraw-Hill series in mechanical engineering, McGraw Hill, 2011.
- [3] B. Munson, A. Rothmayer, and T. Okiishi, *Fundamentals of Fluid Mechanics, 7th Edition*. John Wiley & Sons, Incorporated, 2012.
- [4] J. F. Thorpe, “On the momentum theorem for a continuous system of variable mass,” *Am. J. Phys.*, Vol. 30, 1962, pp. 637–640.
- [5] M. B. Quadrelli, J. Cameron, B. Balaram, M. Baranwal, and A. Bruno, “Modeling and Simulation of Flight Dynamics of Variable Mass Systems,” 2014.
- [6] M. I. Marmureanu and I. Fuiorea, “Attitude Dynamics of a Spinning Rocket with Internal Fluid Whirling Motion,” *INCAS Bulletin*, Vol. 6, No. 2, 2014, p. 75.
- [7] F. O. Eke, “Dynamics of variable mass systems,” 1998.
- [8] H. Schaub and J. L. Junkins, *Analytical Mechanics of Space Systems*. Reston, VA: AIAA Education Series, 3rd ed., 2014, 10.2514/4.102400.
- [9] C. Bruccoleri and D. Mortari, “MRAD: Modified rodrigues vector Attitude determination,” *The Journal of the Astronautical Sciences*, Vol. 54, No. 3-4, 2006, pp. 383–390.